ETP ion detect

ETP Ion Detection Products for Mass Spectrometry

ELECTRON MULTIPLIERS

General Technical Information

PRODUCT DATA

14DM467 500ps MagneTOF® Plus

MagneTOF® detectors provide an exceptional combination of performance characteristics. They eliminate the compromises associated with other TOF detector technologies.

The high performance version, 14DM467, typically achieves single ion pulse widths of <500ps FWHM.

Special attention has been given to minimizing jitter so that pulses from multiple ion events have nearly the same width as single ion events.

Specifications

Model Number	14DM467 Rev. H
Mechanical envelope size (nominal)	45 X 52 X 96 mm (not including mounting tabs)
Input aperture size (nominal)	15 X 33 mm
Single ion pulse width (FWHM)	<0.55 ns Measured at detector output with 3 GHz oscilloscope
Ring after main pulse (typical)	2% measured at detector output with 3 GHz oscilloscope
Maximum sustained linear output current	6 µA for dispersed or spatially concentrated ion beams
Maximum linear pulse height	2.5 Volt into a 50 Ohm load
Maximum dark counts @ 2600V	< 50 per minute
Recovery time after large pulse	Negligible
Maximum operating pressure	10^{-4} Torr
Long/short term storage requirements	Protect from dust in original packaging or in an appropriate desiccator
Maximum current draw from HV power supply at the maximum operating Voltage	0.5 mA
Ambient temperature range for normal operation	15 to 28 °C (59 to 82 °F)
Ambient temperature range for optimum operation	19 to 23 °C (66 to 73 °F)
Typical gain when multiplier is new	1E6 @ ~ 1950V
Operating voltage range*	~ -1800V (initial) to -3400V maximum (aged).

*Note: Operating a new detector at end-of-life (maximum) voltage may result in damage to the detector

ETP ion detect

14DM467 Mechanical Specification

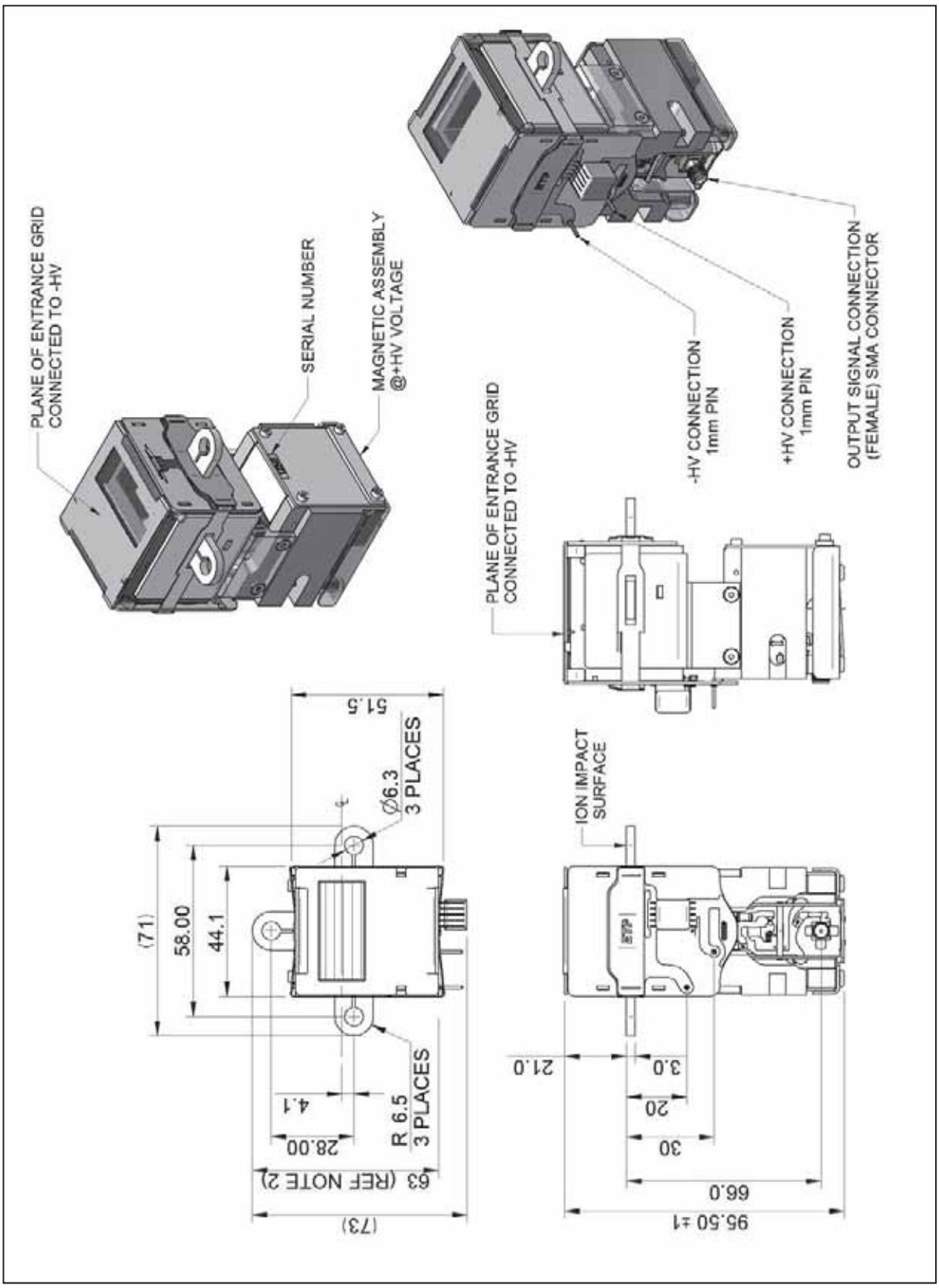

PRODUCT DATA

14DM497 MagneTOF® Mini

MagneTOF® detectors provide an exceptional combination of performance characteristics. They eliminate the compromises associated with other TOF detector technologies.

With a multiple ion pulse width of ~1.5ns, the 14DM497 is a cost-effective detector for systems that do not require the speed of ETP's higher-performance MagneTOF® models.

Specifications

Model Number	14DM497
Multiple-ion pulse width (FWHM)	≤1.5 ns
Input aperture size (nominal)	25 X 17 mm
Mechanical envelope size (nominal)	59 X 55.5 X 45 mm
Pulse linearity (typical)	500 mV into 50 Ω
Maximum sustained linear output current (typical)	5 µA
Maximum dark counts at 2600 V	20 per minute
Maximum dark current at 2600 V	1 pA
Maximum operating pressure	10^{-4} Torr
Long/short term storage requirements	Protect from dust and humidity
Maximum supply current	300 µA
Typical gain at 2000 V	1 X10^{6}
Operating voltage range*	~1900 V (initial) to 3500 V (aged)

*Note: Operating a new detector at end-of-life (maximum) voltage may result in damage to the detector

ETP ion detect

14DM497 Mechanical Specification

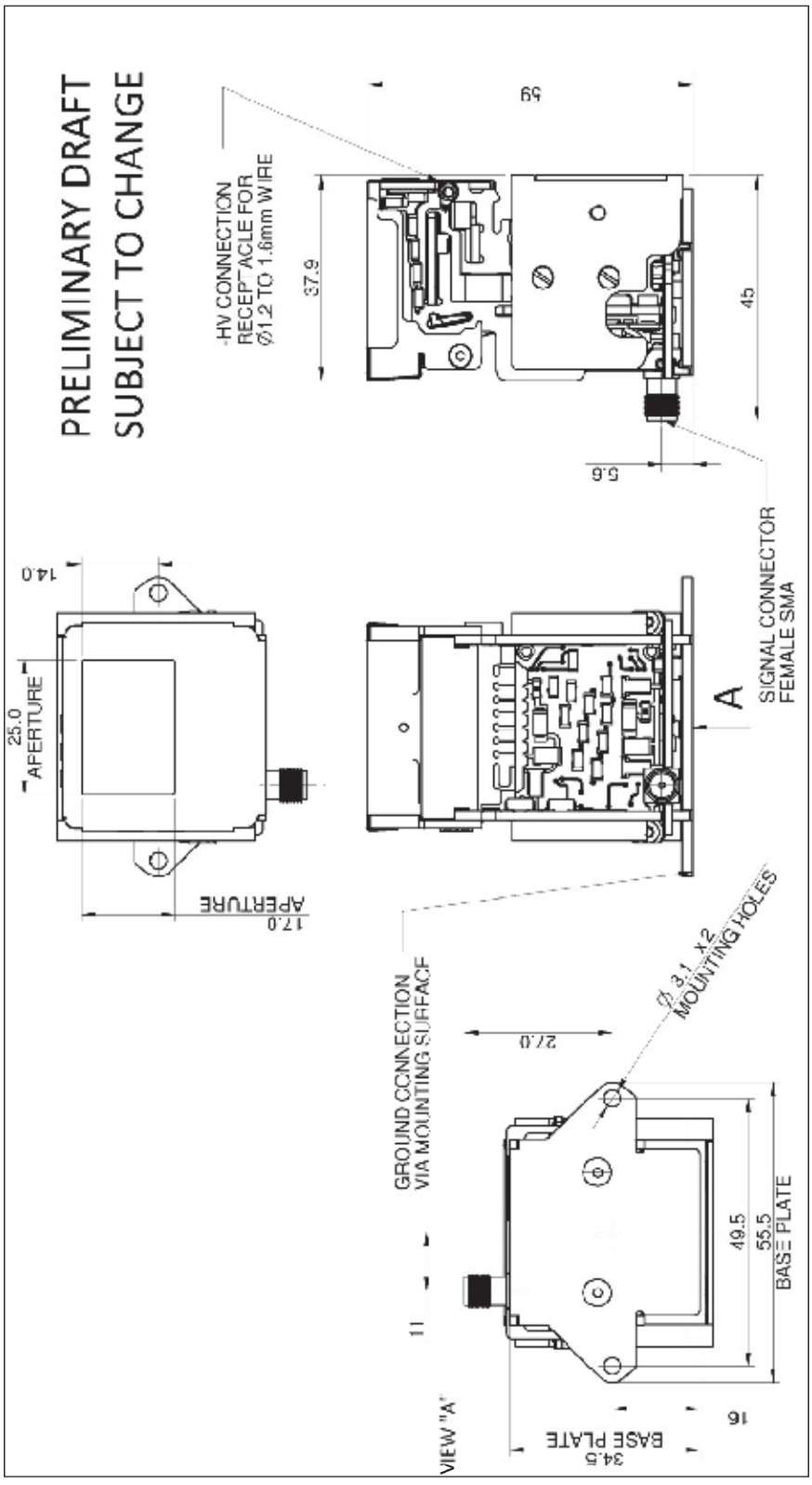

PRODUCT DATA

14DM540 DyneX® RGA Detector

The 14DM540 is a compact discrete-dynode detector designed for applications where the available space is limited. With an integral Faraday cup to extend the dynamic range, it is ideally suited to RGA detection.

The 14DM540 uses an ETP design advance that allows the multiplying section of the detector to be non-linear.

Specifications

Model Number	14DM540
Input aperture diameter (nominal)	6 mm
Mechanical envelope size (nominal)	47L X 35W X 51.2H mm
Number of dynodes	20
Total resistance	22.8 MΩ
Maximum operating pressure	10^{-4} Torr
HV for 1E5 gain (typical)	1550 V
Maximum dark counts at 2500 V	3 counts/min
Maximum dark current at 2500 V	1 pA
Maximum sustained linear output current (typical)	10 µA
Long/short term storage requirements	Protect from dust and humidity
Electrical connections (via 0.6 mm diam. wire)	-HV Ground Signal Faraday cup (connected to signal)
Maximum recommended applied voltage*	3200 V

*Note: Operating a new detector at end-of-life (maximum) voltage may result in damage to the detector

ETP ion detect

14DM540 Mechanical Specification

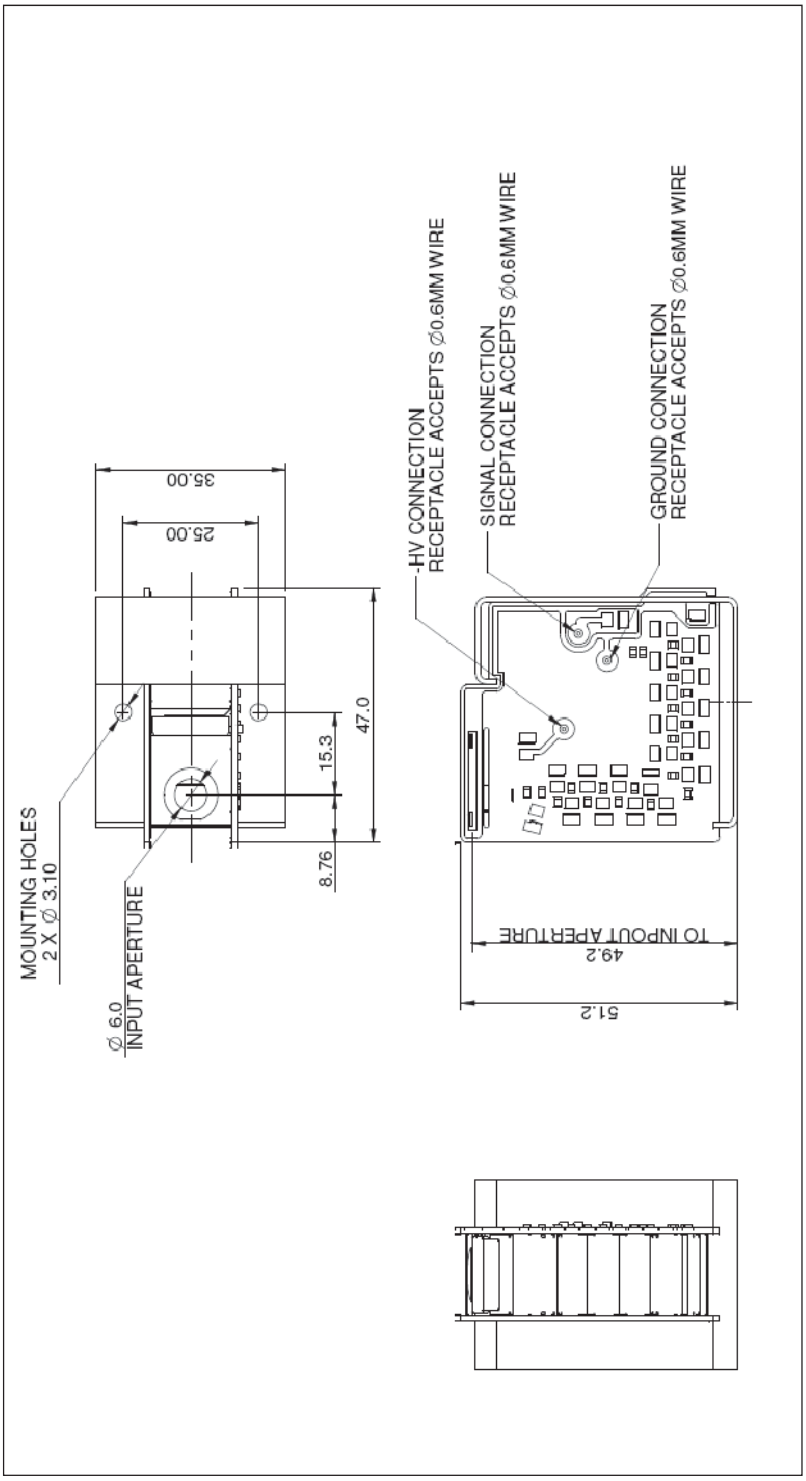

PRODUCT DATA

14DM493 Dual-Mode ICP-MS Detector

The 14DM493 is a high-dynamic range discrete dynode detector designed to meet the demands of ICP-MS instruments.

The 14DM493 uses ETP's dual-mode technology where the first section of the detector operates in analog mode, and is always active, providing a continuous monitor of the ion signal. The second section of the detector provides additional gain to the signal and is used in the pulse-counting mode.

At intermediate signal levels, the pulse-counting and analog sections simultaneously provide signal outputs that are proportional to the input ion current.

Specifications

Model number		14DM493
Input aperture diameter: (nominal)		Ø11mm
Internal resistance: (nominal)	-HV to Gnd +HV to Gnd Gate to Gnd	22.3 MΩ 18.6 MΩ open circuit
Number of dynodes		26
Typical analog gain (new multiplier) (-HV @ -1800 Volts and +HV @ +1000 Volts)		>2.5x10^3
Typical pulse-counting gain (new multiplier) (-HV @ -1800 Volts and +HV @ +1000 Volts)		>1x10^7
Gain Attenuation of pulse-counting section (with gate set to 0V)		> 4000
Maximum analog dark current (-HV @ -2500Volts and +HV @ +1000 Volts)		<1 pA
Maximum pulse-counting dark counts (-HV @ -1800Volts and +HV @ +1400 Volts)		≤ 3 counts per minute
Maximum operating pressure		10^{-4} Torr
Electrical connections		- HV +HV Gate Analog output Pulse output
Maximum applied bias voltages*	-HV +HV	- 3000 Volts +2500 Volts

* Maximum multiplier voltage must not be applied to a new multiplier, or damage to the multiplier may result. Maximum multiplier voltage should only be applied to the multiplier when it is near end of life.

ETP ion detect

14DM493 Mechanical Specifications

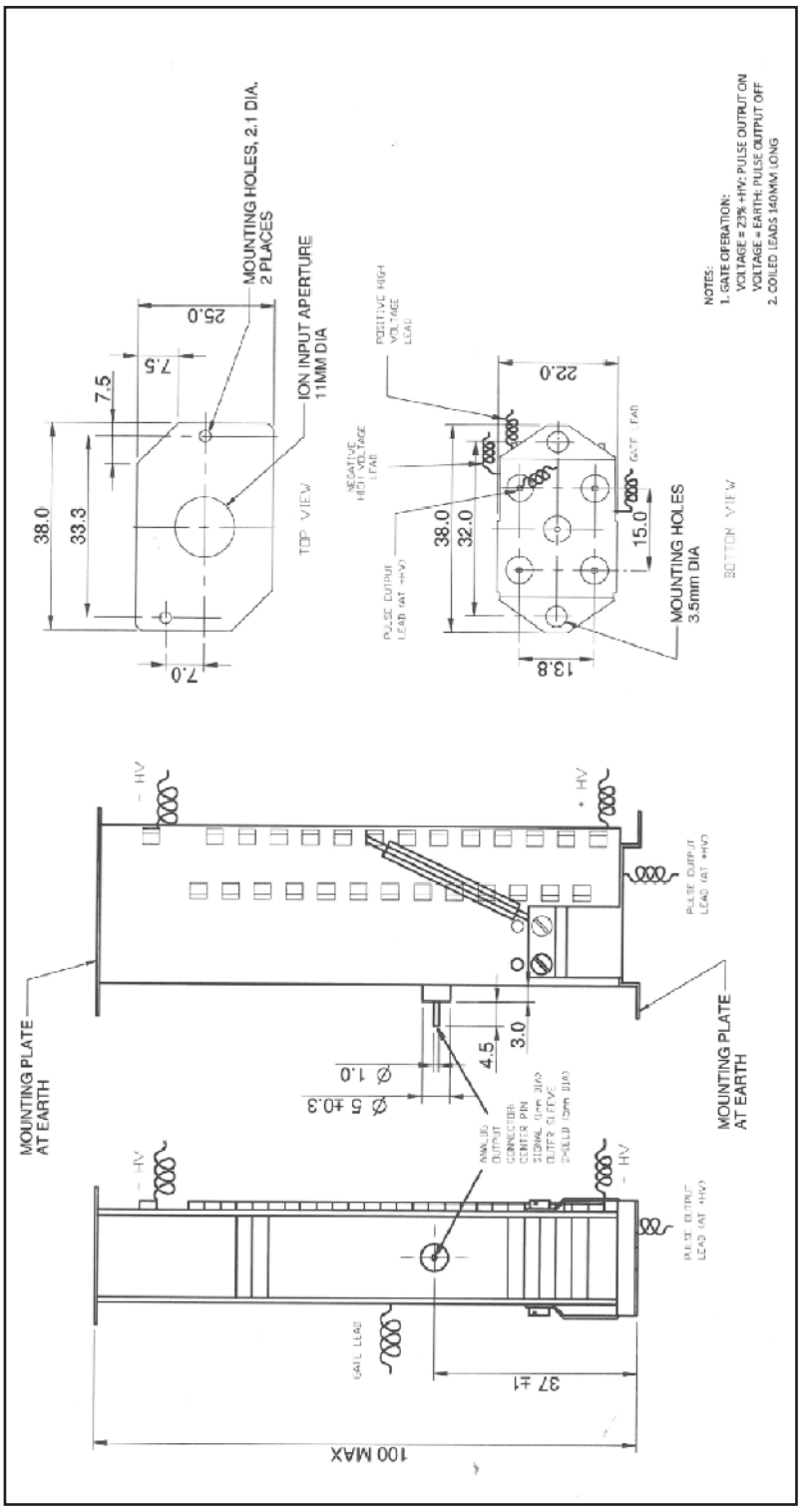

PRODUCT DATA

HIGH ENERGY DYNODE DETECTOR FOR ION TRAPS AND QUADRUPOLES

Preliminary Data sheet - Specifications may change

- **High Detection Efficiency for Ion energies from 1 eV to 5 keV**
- **Suitable for both Ion Traps and Quadrupoles**
- **± 10 kV HED Operation**
- **Positive and Negative Ion Detection**
- **Snap-in multiplier section**

This unique high energy dynode (HED) multiplier is designed to be sensitive to a very wide range of ion energies. While this is critical for ion trap operation, it will also enhance the performance of quadrupole systems operating at high mass. Therefore, it is ideal for LC-MS applications.

As in all HED multipliers, a high voltage (± 10 kV) is applied to the conversion dynode (HED) to accelerate the ions before their interaction with the dynode surface. This enhances the electron (or secondary ion) yield from the dynode, which is particularly important for high mass ions which have inherently low yield. For negative ion detection, positive high voltage is applied to the HED and the secondary positive ions generated from the initial ion impact are focussed into the amplifying section. For positive ion detection, negative high voltage is applied to the HED and secondary electrons generated from the ion impact are focussed into the amplifying section.

Three different models are available; each featuring very efficient ion optics. Refer to **Table 1** for details of mechanical size and operational lifetimes.

All ETP electron multipliers incorporate totally air-stable "ACTIVE FILM" materials in a discrete-dynode multiplier design to achieve exceptionally sensitive ion detection with long operating life and excellent air stability.

ETP ion detect

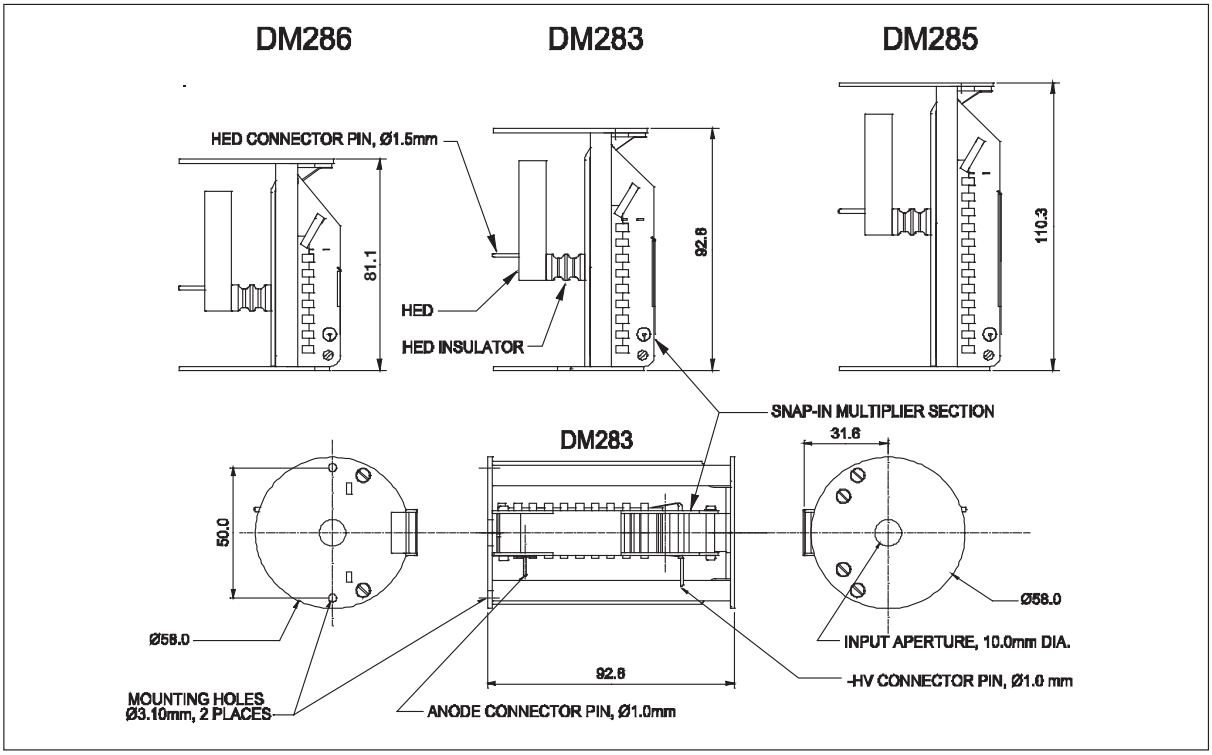

Table 1 - *Technical Specifications*
* The operational life figures are based on simulation and are an indicator only.

Specifications	DM286	DM283	DM285
Sensitive area (mm)	10mm dia.	10 mm dia.	10 mm dia.
Maximum noise when operated at 2500 V.	< 1 pA	< 1 pA	< 1 pA
Relative life expectancy*	100% @ 3.0kV max	150% @ 3.0kV max	300% @ 3.5 kV max. 450% @ 4.0 kV max.
Overall length	81.1 mm	92.8 mm	110.3 mm
Maximum recommended applied voltage	3.0 kV	3.0 kV	4.0 kV
Recommended HED voltage	± 10 kV	± 10 kV	± 10 kV
Internal resistance	23 MΩ	28 MΩ	37 MΩ
Number of dynodes	15	19	25

PRODUCT DATA

14DM482 HED DETECTOR

The 14DM482 HED detector assembly is a high dynamic range detector for quadrupole GC-MS Instruments. The assembly is designed so that the multiplier is a clip-in replacement unit that can be replaced in a few minutes with no tools required.

Three new concepts utilized in the 14DM482 lead to superior signal to noise performance:

- The ion trajectories are rotated through 270^0 onto the HED leading to a major reduction in noise from radiation and neutrals.
- An Einzel collimator efficiently transfers ions to the HED region through small diameter holes which minimize the passage of radiation and neutrals, further reducing noise.
- Ions strike the HED surface at a grazing angle, 60^0 from normal, increasing the secondary yield by up to X2 with a comparable increase in ion detection efficiency for high masses.

This detector includes a Mount Assembly incorporating the HED, which is permanently bolted to the instrument.

Electrical connections are:

- HED, via a 1mm diameter pin,
- Lens, via a 1mm diameter pin,
- Multiplier HV, via a 1mm diameter receptacle, and
- Output signal, via a 1mm diameter pin

Separate leads are required for these connections, and can be designed and manufactured by ETP as required.

ETP multipliers incorporate air-stable “ACTIVE FILM” materials in a discrete dynode multiplier design to achieve exceptionally sensitive ion detection with long operating life and excellent stability in air.

14DM482 Draft Detector Specifications

Input aperture (mm)	6mm dia, nominal
Voltage Divider : Resistance total (nominal) Zener Total (nominal)	10.2MΩ (nominal) 133V (nominal)
Number of dynodes	17
Maximum recommended bias voltage	3500V
Maximum sustained output current for linear operation	35µA
Recommended Lens Voltage	±600V
Maximum HED Voltage	±10kV
Maximum dark counts (-HV @ -2500V, HED @ -10kV	< 20 counts per minute
Maximum analog dark current (-HV @ -2500V, HED @ -10kV)	<1pA
Maximum operating pressure	10^{-4} Torr

ETP ion detect

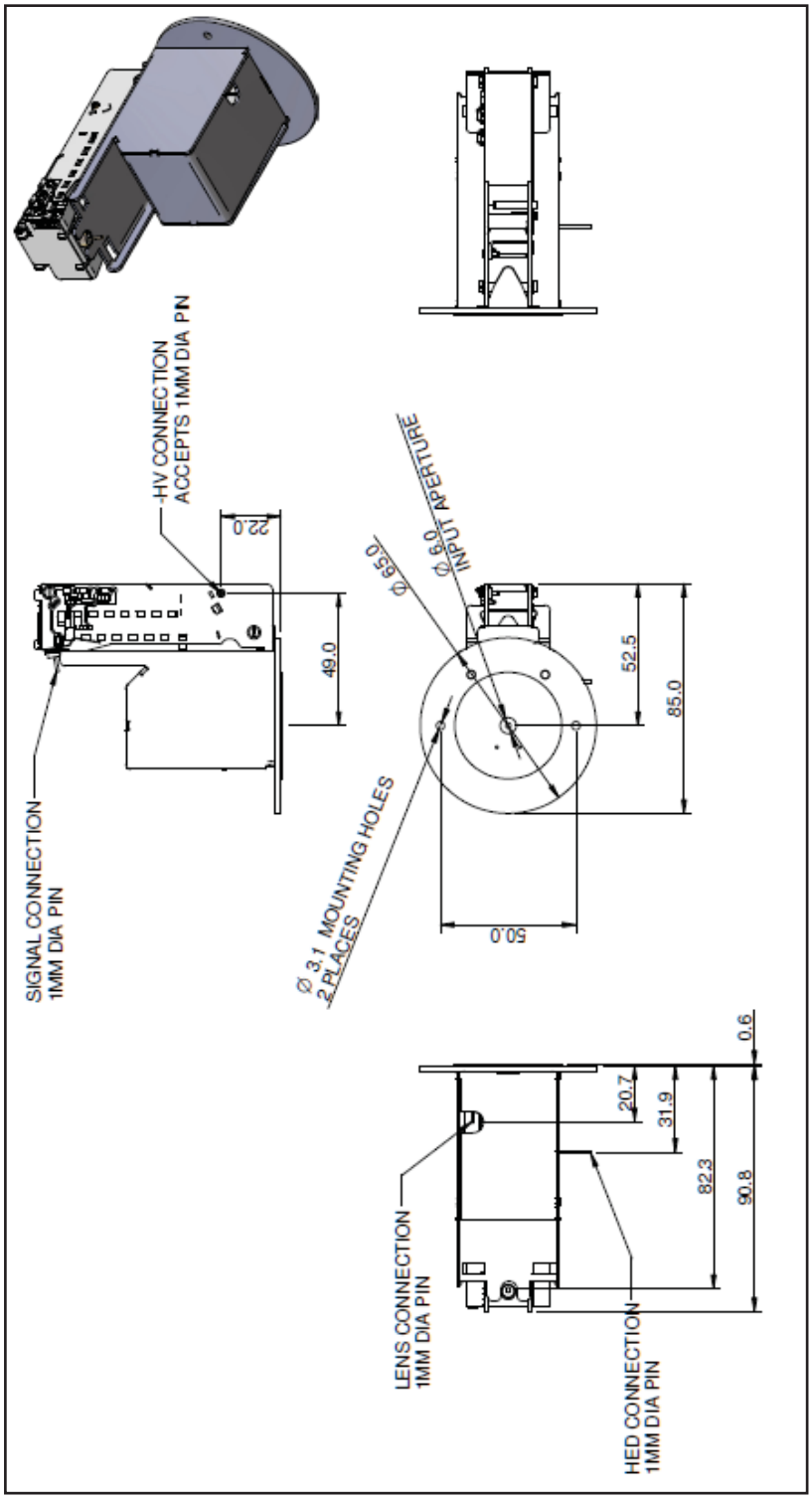
HV CONNECTION
ACCEPTS 1MM DIA PIN
22.0
49.0
SIGNAL CONNECTION
1MM DIA PIN
Ø 65.0
Ø 6.0
INPUT APERTURE
52.5
85.0
Ø 3.1 MOUNTING HOLES
2 PLACES
50.0
0.6
20.7
31.9
82.3
90.8
LENS CONNECTION
1MM DIA PIN
HED CONNECTION
1MM DIA PIN

PRODUCT DATA

GrideX® Ion Optical Grids for Applications in Time-Of-Flight Mass Spectrometry

- PARALLEL WIRE GRID
- 18µm TUNGSTEN WIRE CONSTRUCTION
- 92% TRANSMISSION (250µm PITCH)
- EXTREMELY RUGGED AND DAMAGE RESISTANT
- CIRCULAR OR RECTANGULAR UP TO 180mm
- CERAMIC OR METAL FRAMES
- CUSTOMIZATION CAPABILITY AVAILABLE

ETP introduces its GrideX® range of parallel wire analytical grids. Developed to facilitate the high-speed performance of ETP's latest range of TOF detectors, the grids are also applicable to ion and electron optics.

The grids are ideal for application as field isolation and termination elements in both linear and reflectron instruments. They may be incorporated in sources, analyzers and anywhere a high transmission, flat grid structure is required.

Constructed from high strength tungsten wires, ETP grids are extremely rugged in comparison to similar products fabricated from photo-etched mesh materials. This ruggedness makes them less prone to damage from handling, or during instrument manufacture. The parallel wire design allows a specified grid transmission to be held to a high tolerance. The wires of the standard grid are 18 µm tungsten at a pitch of 250 µm, giving a transmission of 92%.

ETP ion detect

Typical Grid Configuration

The rugged tungsten wire construction of ETP's grids eliminates the warping and bowing often seen with photo-etched mesh material.

ETP ion detect

TECHNICAL ARTICLE

A New Class of Robust Sub-nanosecond TOF Detectors with High Dynamic Range

Dick Stresau, Kevin Hunter, Wayne Sheils, Peter Raffin and Yair Benari

ETP, Sydney, Australia

Presented at the 54th ASMS Conference on Mass Spectroscopy, Seattle, Washington, 2006

Four years ago ETP had the vision to develop a superior TOF detector. The project objectives were very simple:

- Less than 1 nanosecond pulse width
- To retain all of the advances in TOF detector technology ETP has made during the past several years (reported in various presentations to this meeting)

The result of this work is the new MagneTOF™ detector. Figure 1 shows the pulse shape from the new detector showing the typical pulse width of ~400 ps.

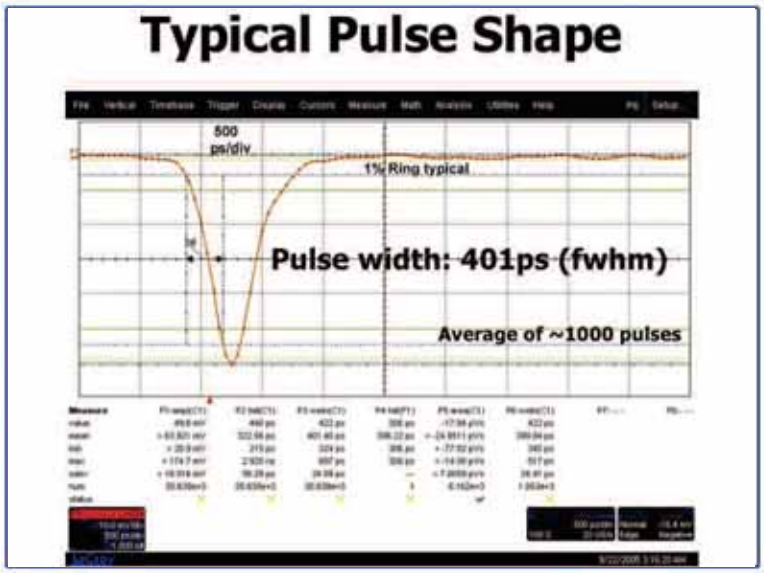

Figure 1: *The typical pulse shape obtained using the DM167 MagneTOF™ electron multiplier.*

It clearly exceeds our initial objectives. Notice that the ring is minimized to ~1%.

ETP TOF detectors have become the preferred detector for many applications during the past 14 years because of their advantages over the alternative MCP detectors. These distinguishing advantages were included in the design objectives for the MagneTOF™ and are summarized:

- High linear pulse output current
- High linear sustained output current
- Fast recovery after ion burst
- Full performance immediately after pump-down
- High pressure operation
- Low noise
- Long life
- Robust construction

The most useful and important features are the detector's linearity at high signal levels and its ease of use.

Until now wide pulse width has been the only limitation for ETP TOF detectors, limiting their use in a number of applications. To overcome this limitation a number of new technologies were developed.

The key technology for achieving very narrow pulse widths has been the use of magnetic deflection for inter-dynode electron transfer.

ETP ion detect

The diagram in Figure 2 could have been taken from a first year physics text book. It shows the near toroidal trajectories of charged particles in crossed magnetic and electrostatic fields. In this diagram the particles have initial velocities expected from secondary electrons (generated from ion or electron impact).

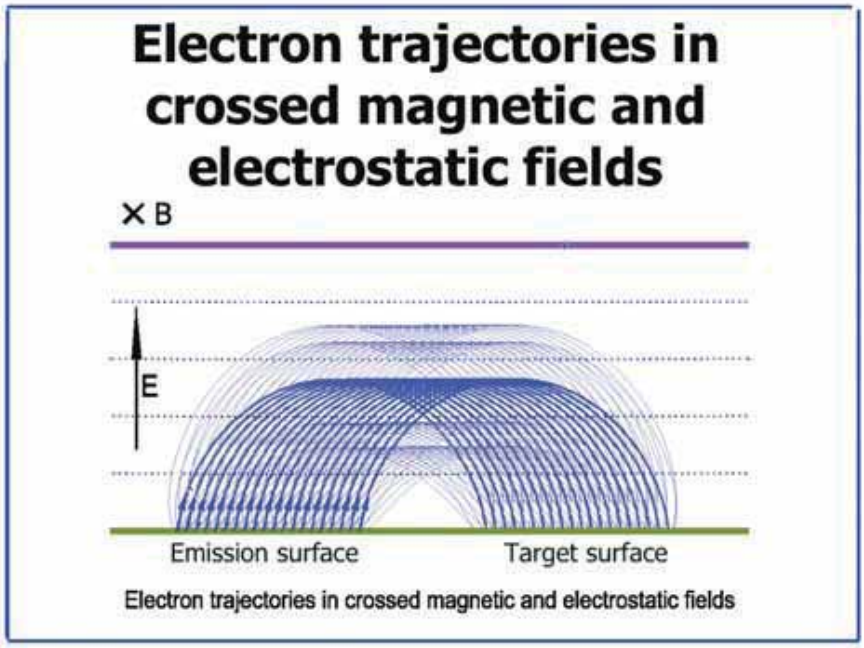

Figure 2: *Electron trajectories in crossed magnetic and electrostatic fields.*

There are a number of very useful characteristics of this process that are not immediately apparent. The most "magical" of these is the almost total lack of time distortion in electron transit times from the emission surface to the target surface. In near uniform magnetic and electrostatic fields (as used in the amplifying section of the new detector) inter-dynode electron time dispersion is on the order of 10 picoseconds.

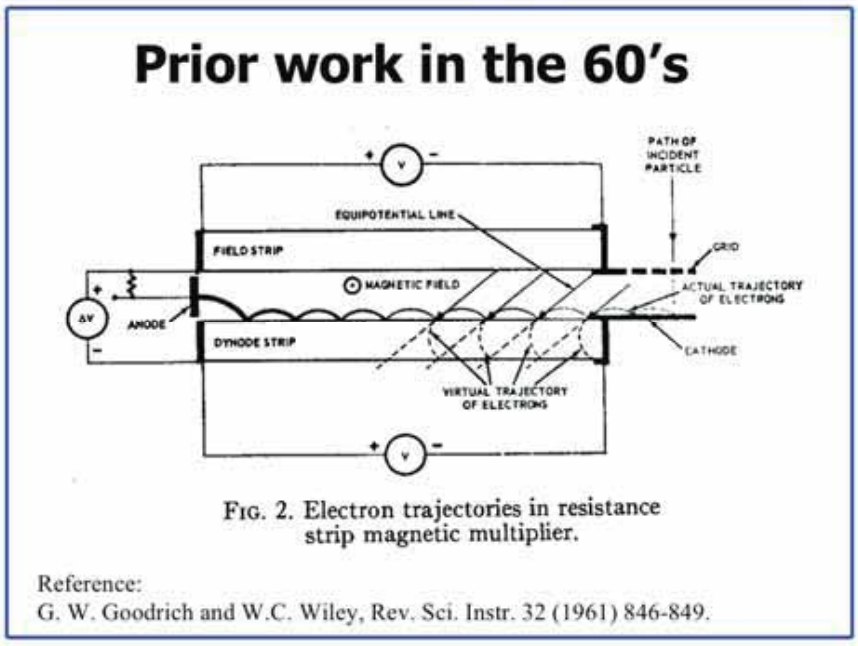

Figure 3: *Earlier work in the field by Goodrich and Wiley.*[1]

We are not the first group to use these concepts in a particle detector. In the early '60's the very prolific Bendix group developed these concepts into a commercial detector. (Figure 3)[1] This was the same group that developed the first commercial TOF system, the channeltron detector and the MCP.

The significant drawback of this early design was that each individual dynode surface must be the same size as the input aperture. A useful detector of this design using today's input aperture requirements would be so large as to be impractical. This limitation has been overcome by utilizing non-uniform magnetic fields.

Two important things have changed since the 1960's to make this basic approach practical once again:

- The need for a very fast particle detector
- Easily accessible, very powerful computers: - PCs

Figure 4 shows ETP's solution to the need for computing power. It's a cluster of 8 PC's which gives us the equivalent computing power of a "20 GHz Pentium". It enables the analysis and development of very complex magnetic and electrostatic structures fast enough to enable interactive modeling.

Figure 4: *ETP's cluster computer - a solution to the need for powerful computing for modeling*

Figure 5 shows the basic optics arrangement of the new detector. The thick black lines show the basic mechanical structure and green lines electrostatic equipotentials. The red lines indicate input ion trajectories and the blue lines secondary electron trajectories.

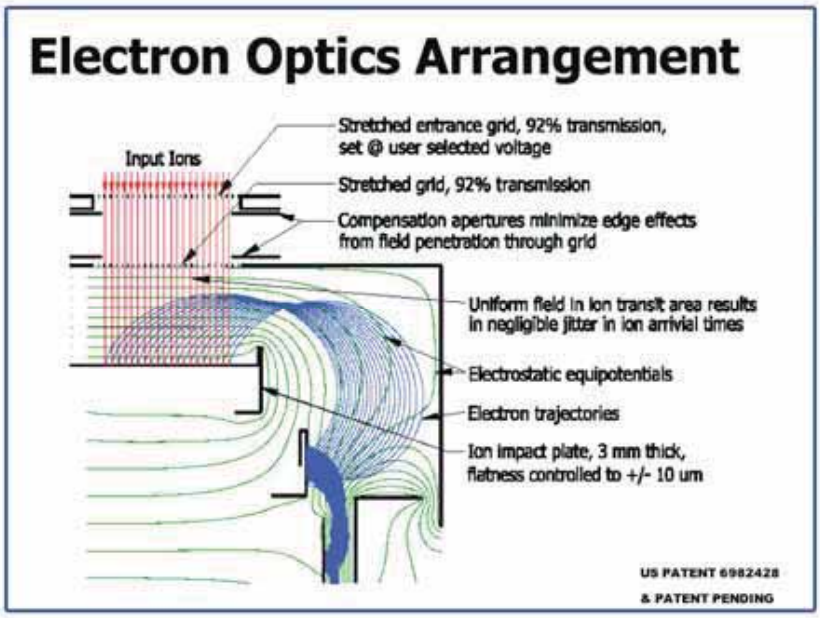

Figure 5: *The electron optics arrangement for DM167 MagneTOF™.*

It's worth pointing out a number of features:

1. An outer grid, which can be fixed at a user-defined voltage (within ±5 kV of the applied -HV), is included in the design for ease of integration into a TOF system.

2. The ion input grids are made from parallel wires stretched over a flat frame enabling precision control over transmission to 92%.

3. To take advantage of narrow pulse width it is important to minimize jitter and arrange for minimum disturbance to the input ions as they pass through the detector to the impact surface. To achieve this:

a. A significant effort has been given to design for a very uniform electrostatic field in the ion transit area. The small "kick-up" at the right end of the ion impact plate is an example of the design details included to achieve this goal.

b. Each internal transmission grid is equipped with a compensation aperture which compensates for edge effects from field penetration through the grid.

c. The ion impact surface is made from 3 mm thick stainless steel (coated with appropriate dynode materials). This allows for an unusually flat ion impact surface: ±10 micrometers is standard, ±5 or smaller is optional.

d. The grids are made from parallel wires stretched over a flat frame enabling very flat grid surfaces.

Figure 6 is a view of the optics, showing contour lines of equal magnetic field strength in blue and red. This clearly shows the complex non-uniform nature of the magnetic field. This non-uniform field focuses the electrons from the large ion impact surface to the smaller second dynode, as seen from the electron trajectories in green.

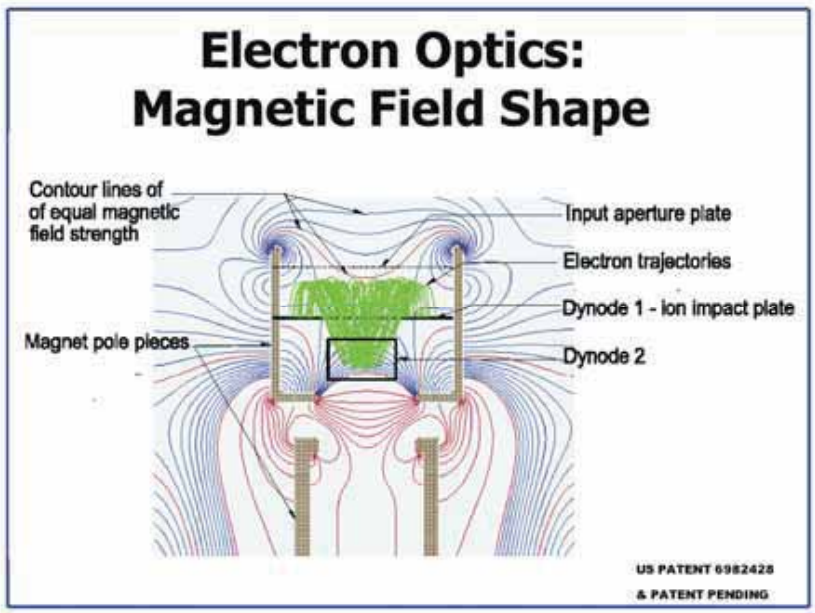

Figure 6: *A view of the optics of DM167 MagneTOF™, showing the magnetic field shape*

Figure 7 shows an example of the simulations arranged to analyze the time distortion or jitter resulting from aperture edge effects and field penetration through the entry grids. It was necessary to carry out the simulation with a 6 micrometer array spacing to achieve accurate results.

Because these are ion arrival times the results are dependant on the ion's mass and energy. The analysis was done with 5 keV, 10,000 amu ions as a worst case scenario. Small, energetic ions will have negligible jitter.

This type of analysis was used to determine the optimal voltages to be applied to the compensation apertures to achieve minimal distortion.

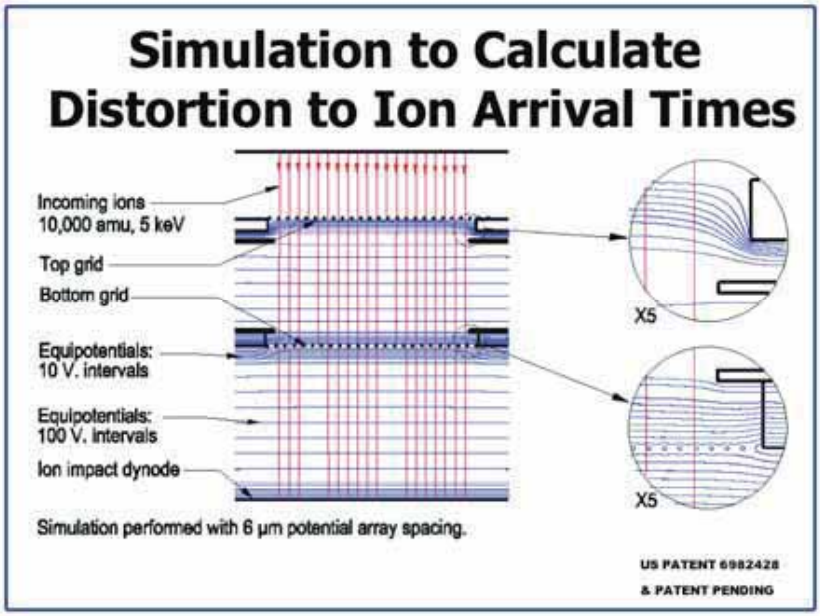

Figure 7: *An example of the simulations arranged to analyze the time distortion resulting from aperture edge effects and field penetration*

Figure 8 shows results from the distortion analysis showing ion arrival time as a function of position on the ion impact surface. There is less than 50 picosecond jitter across the surface except at the very edges of the aperture where it reaches ~100 picoseconds. Note that "DM167" is the version number given to the MagneTOF™ detector used to collect this data.

The outer grid of the detector can be set to an arbitrary voltage selected by the user (within ± 5 kV of the applied -HV). This analysis was done with the outer grid attached to the detector's -HV.

Figure 9 shows the same analysis, but now the outer grid is set at the detector's +HV potential or earth for non-floating applications.

Note again that the analysis was carried out with worst case conditions of 10,000 amu ions with 5 keV energy.

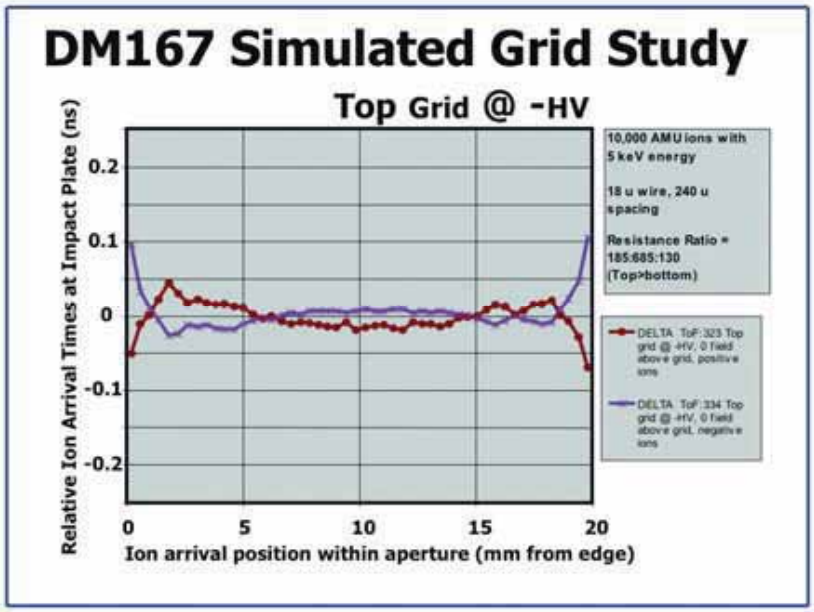

Figure 8: *The results from the distortion analysis showing ion arrival time as a function of position on the ion impact surface (outer grid attached to the detector's -HV)*

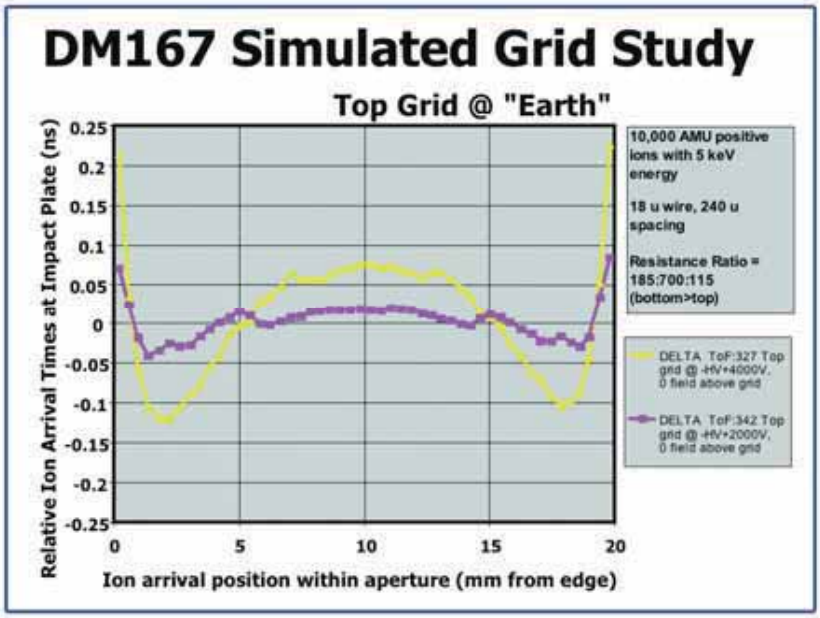

Figure 9: *The results from the distortion analysis showing ion arrival time as a function of position on the ion impact surface (outer grid attached to the detector's +HV, or earth for non-floating operation).*

The most realistic exercise devised for this detector in our lab is the "ion burst test". It is a realistic measure of the performance one can expect from this detector during a very high abundance TOF spectrum (Figure 10).

For this investigation the detector was exposed to 5 microsecond bursts of ions with a 1% duty cycle. The incident ion rate was increased until a variation of multiplier gain was observed during the ion burst. The lower trace is the average of ~2500 ion bursts and hence indicates the average detector output current, and therefore instantaneous detector gain, during the burst.

The calculations on Figure 10 show how this data corresponds to linear response during an ion burst of 300,000 ions.

The detector's averaged output of 30 mV (or 600 µA into 50 Ohms) during the 5 microsecond burst is the equivalent of an ion input rate of 6 X 10^{10} ions per second (for 1 mV single-ion-pulses). This corresponds to a total of 300,000 ions during the burst. From the data it is apparent that this ion burst rate has negligible influence on detector gain for the first microsecond followed by a minor gain increase (corresponding to the detector's over response at very high currents).

Work is continuing in this area and it is anticipated further improvement in the ion burst performance of the MagneTOF™ detector will be achieved.

Figure 11 shows a real example of serendipity. The objective was to achieve an operational life equivalent to that of "standard" ETP electron multipliers. The observed aging rate is considerably lower than any previous ETP electron multiplier or that reported for any electron multiplier.

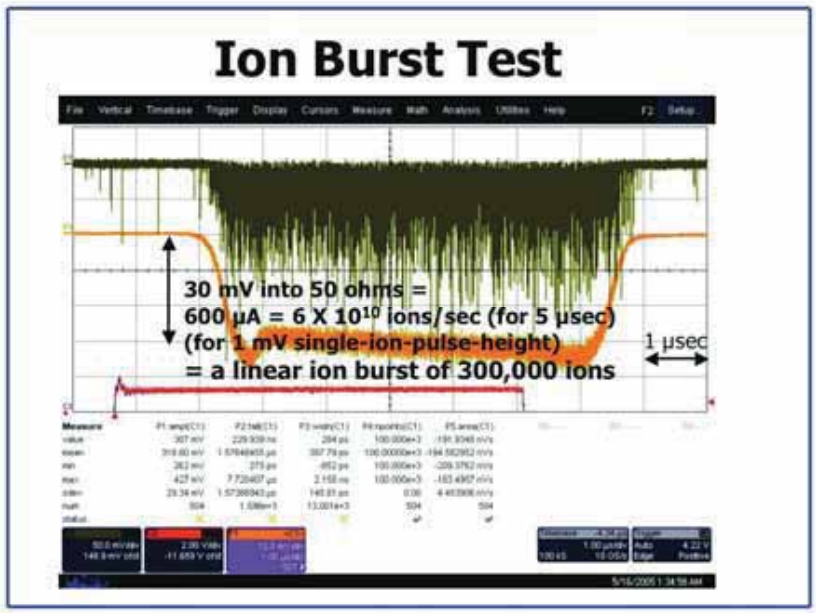

Figure 10: *The ETP ion burst test is a realistic measure of the performance that can be expected from the DM167 MagneTOF™ detector during a very high abundance TOF spectrum acquisition.*

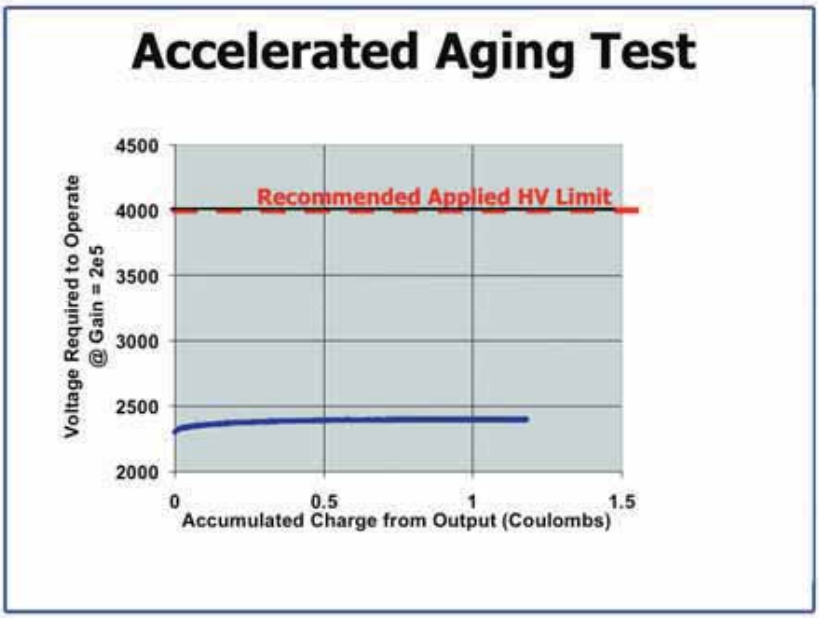

Figure 11: *An aging test shows that the DM167 MagneTOF™ multiplier lifetime is far greater than reported for any other electron multiplier.*

To approximate the expected operating life of the MagneTOF™ it was operated in a system that periodically adjusted the applied high voltage to maintain a gain of 2 X 10^5 (~3 mV single ion pulse height into 50 ohms).

The blue curve shows the voltage required to maintain this gain and indicates negligible aging for >1 coulomb of accumulated output charge.

ETP ion detect

The input ion beam was operated with a 50% duty cycle (50 ms on, 50 ms off) to approximate somewhat normal usage conditions. During the beam-on state the detector output current was maintained at ~10μA (corresponding to ~3X10^{8} ions/second of input ion flux, within the detector's linear operating range). This experiment was conducted in a chamber pumped with a turbo pump-diaphragm pump system to a pressure of 5 X 10^{-6} torr.

Work is continuing on understanding the mechanisms involved in this result and it is expected to be utilized in other application areas.

Figure 12 shows the typical pulse height distribution of the new detector. It has an unusual shape as a result of the very high secondary electron yield from the second dynode. This enables the resolution of individual peaks resulting from the Poisson distribution of the number of secondary electrons generated by ion impact on the first dynode.

The dark blue blocks show the Poisson distribution for a mean of 2.0 events. This is the expected distribution of the number of electrons emitted from an ion impact with an average yield of 2, which is appropriate for the 30 amu, 3 keV ions used to collect this data.

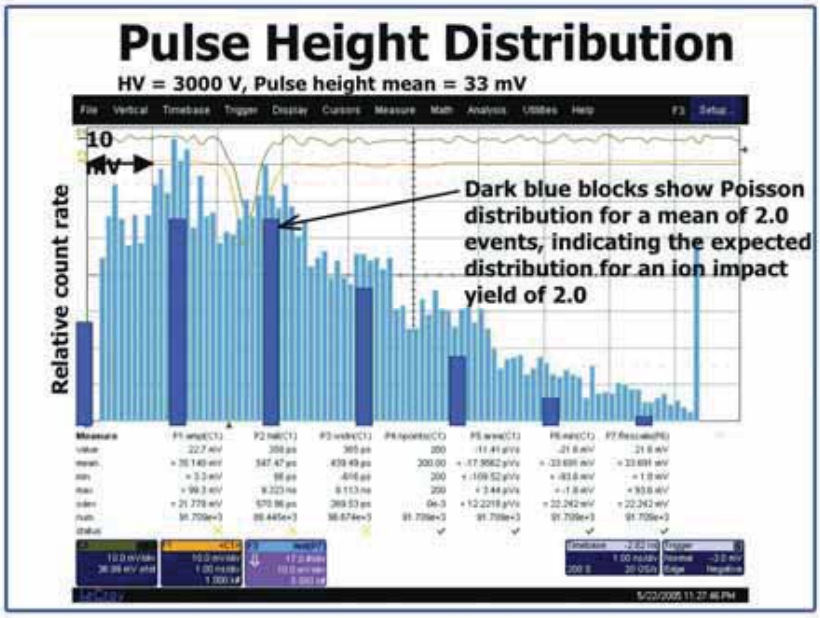

Figure 12: *Typical pulse height distribution of the MagneTOF™ detector*

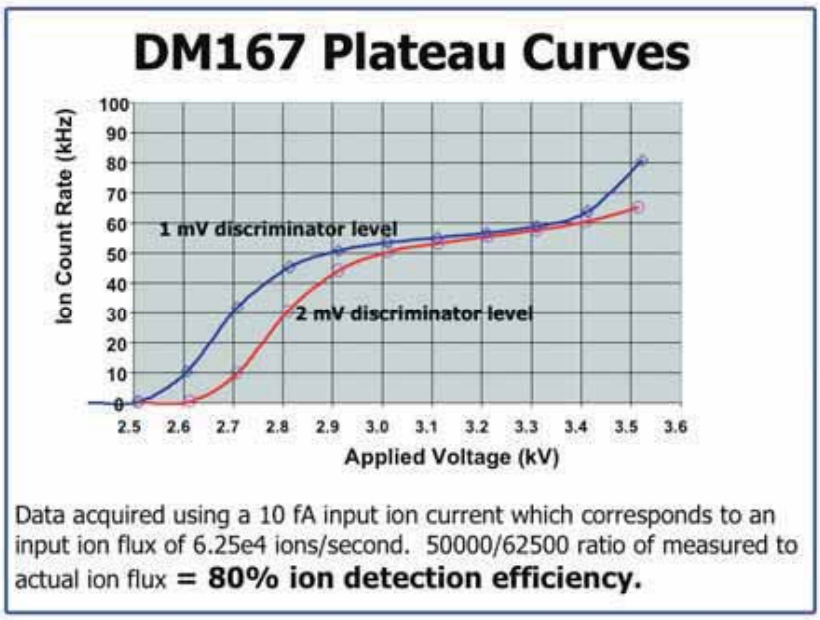

Figure 13: *Plateau curves generated using the new MagneTOF™ detector*

The distribution is dominated by the ion impact secondary yield characteristics and therefore is as narrow as can be expected from a non-saturating detector. A larger yield and thus narrower distribution can be expected from higher energy ions.

Figure 13 shows a plateau curve generated with the new detector using the conventional method of increasing the applied HV in steps and recording the output count rate while exposing the detector to a fixed flux of input ions.

This is the standard method used for setting the appropriate HV for most pulse counting and TOF systems.

When the HV is set to just above the "knee" (~2.9 kV in the 1 mV case) it can be assumed that essentially all of the ions have been detected that have generated pulses within the detector.

The input ion current can also be measured. Converting this to an input ion rate enables calculation
of the detector's absolute ion detection efficiency as the ratio of the two measurements.

Applying this procedure to this data results in an 80% ion detection efficiency, which is very close to the value expected from grid transmission and Poisson statistics.

The detector on the right of the photograph in Figure 14 is the DM167 version of the MagneTOF™, that has been used to collect the data in this paper. To give an idea of scale: its ion entrance aperture, at the top, is 15 X 33 mm.

Following the success with the DM167 a more compact, lower cost version of the detector was designed. The resulting DM291, on the left in Figure 14, has a 10 X 25 mm aperture and has ~1 ns pulse width.

Figure 14: *The MagneTOF™ range of electron multipliers and accessories.*

In the foreground is the DM345 AC Signal Coupling unit, which can be attached to either version and provides 15 kV isolation of the output signal from the rest of the unit.

Summary of the DM167 MagneTOF™ detector's characteristics:

- 400 picosecond pulse width (FWHM)
- Linear response:
  - During and after a burst of 300,000 ions
  - 1 Volt output pulse (into 50 ohms)
  - 10 microamp sustained output current
  - For spatially concentrated ion beams
- Exceptional operating life
- Very flat ion impact surface: ±10 micron (± 5 micron or less optional)
- Full performance just after pump-down
- No special storage requirements

So what is the future for this technology?

How fast can it go?

To get a feel for how well the technology follows the basic design assumptions, a few of the operational parameters were pushed to their extreme.

This resulted in a 250 picosecond pulse width. (Figure 15).

To date no fundamental limits for speed have been reached with the MagneTOF™ detector.

100ps looks achievable if chosen as a design objective.

This may become important for future TOF systems.

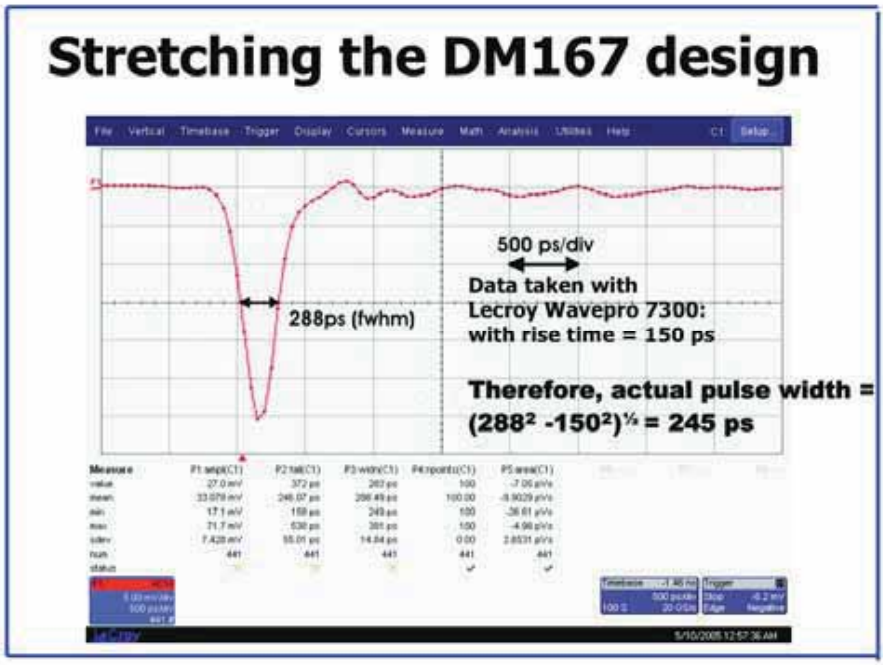

Figure 15: *By pushing various design parameters to their extreme the MagneTOF™ detector achieved a pulse width of 250 picoseconds!*

Conclusions:

- The MagneTOF™ detector exhibits 400 ps pulse width as well as all the dynamic range and robust features of ETP detectors (outlined above).
- The new MagneTOF™ detector eliminates the compromises associated with previous TOF detectors.
- The new technology will continue to meet the demand for ever-increasing TOF detector performance.

Acknowledgements:

Thanks to Hermann Wollnik who offered valuable ideas and insight into many important details at various stages of this project.

References:

1. G. W. Goodrich and W.C. Wiley, Rev. Sci. Instr. 32 (1961) 846-849

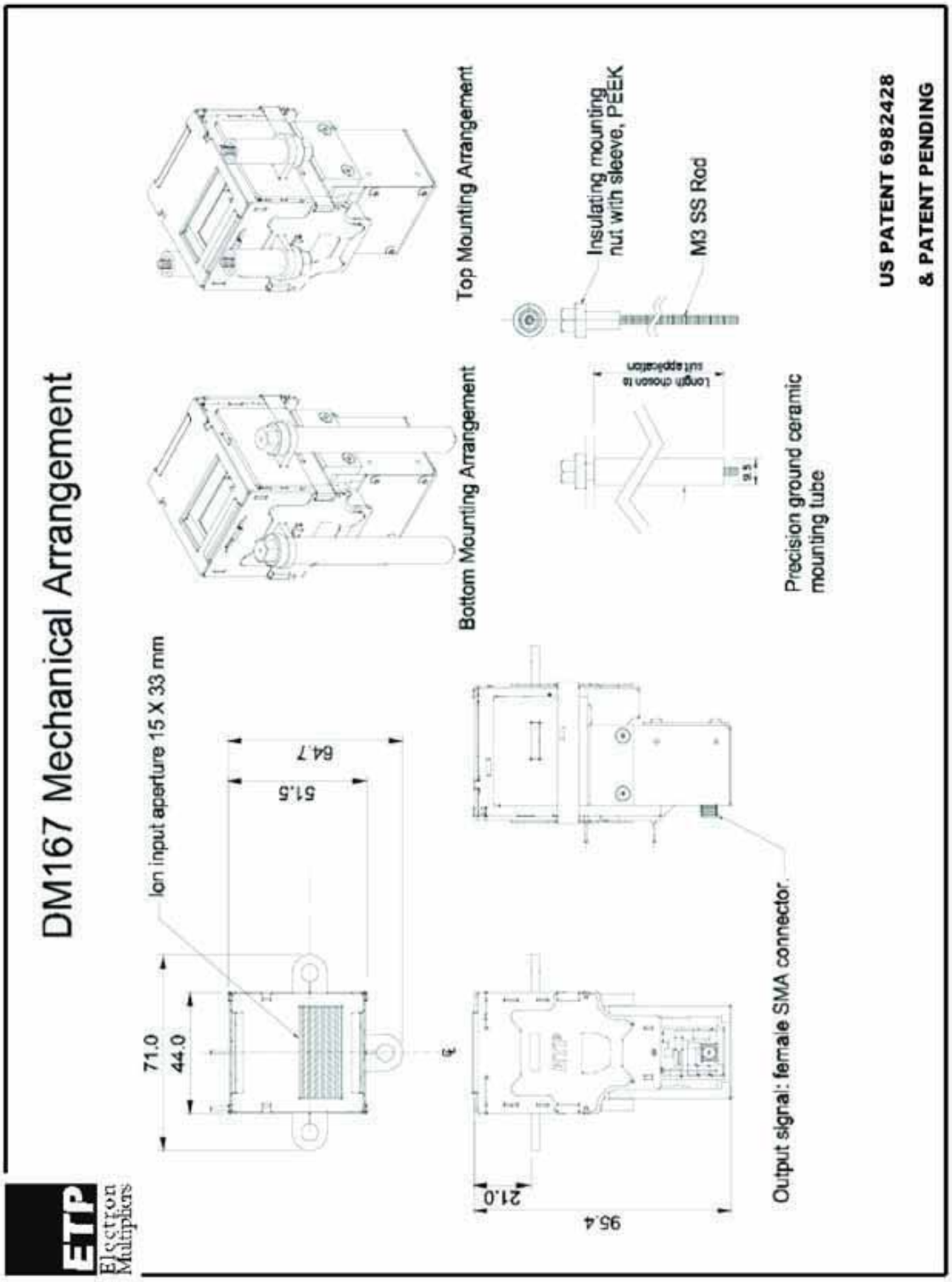

Figure 16: *The mechanical arrangement of the DM167 MagneTOF™ electron multiplier.*

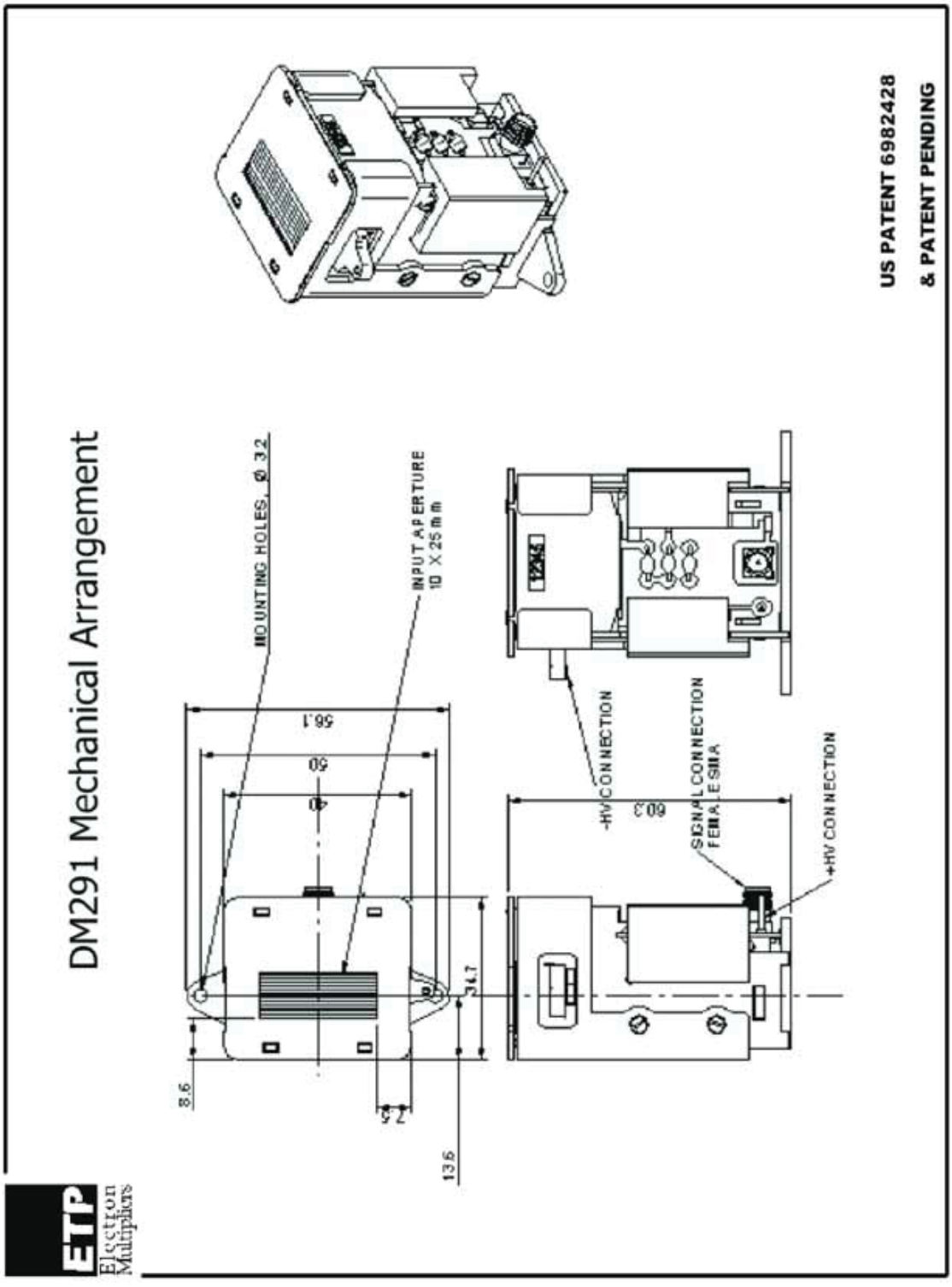

Figure 17: *The mechanical arrangement of the DM 291 MagneTOF™ electron multiplier.*

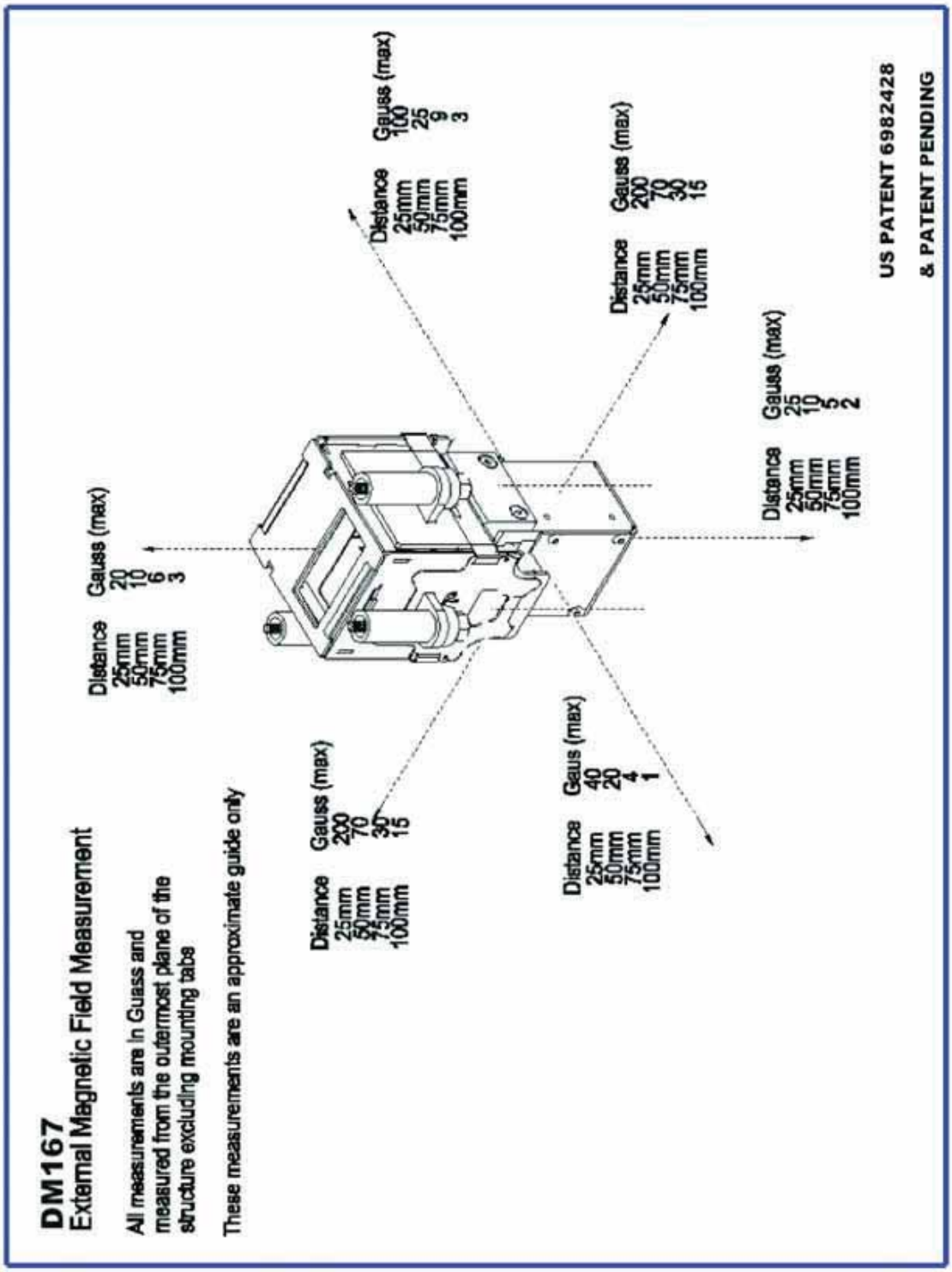

Figure 18: *The external magnetic field measurement of the DM167 MagneTOF™ electron multiplier.*

Table 1.

Specifications	DM167	DM291
Multiple ion pulse width (FWHM) (ns)	<0.5	<1.0
Input aperture size (mm)	15 X 33	10 X 25
Mechanical envelope size (mm) [1]	44 X 52 X 96	38 X 40 X 60
Linear response:	During & after a burst of 300,000 ions	
Linear response:	>1 Volt output pulse (into 50 Ohms)	
Linear response:	10 µA sustained output current	
Linear response:	For spatially concentrated ion beams	
Impact surface flatness:	±10 µm (±5 µm or less optional)	
Maximum dark counts:	20 per minute @ 3000 Volts	
Recovery time after large pulse:	Negligible	
Maximum operating pressure:	10^{-4} Torr	
Long/short term storage requirements:	Protect from dust	
Ion detection efficiency (low mass):	80%	
Conditioning time after pumpdown:	None	
Operating voltage[2]:	~2500 (initial) to 4000 (aged)	
Typical gain at 2500 volts:	10^{5} = ~1 mV into 50 Ohms	

1. Mounting tabs protrude beyond each of these envelope sizes.
2. Up to 0.5 mA will be drawn from the HV power supply.

Table 1: The preliminary specifications for the MagneTOF™ range of electron multipliers

TECHNICAL ARTICLE

SIMULTANEOUS MODE

ELECTRON MULTIPLIER WITH ANALOG AND GATED PULSE-COUNTING OUTPUTS

Dick Stresau and Kevin L. Hunter
ETP Pty. Ltd., Australia
Presented at the 41st ASMS Conference on Mass Spectroscopy and Allied Topics
May 31-June 4, 1993, San Fransisco, California

INTRODUCTION

In some applications of mass spectrometry it is desirable to analyze mass spectra containing peaks which range from less than 100 counts per second (cps) to in excess of 10^9 cps.

This capability is especially desirable in isotope ratio applications where a very large elemental mass peak and a small isotope peak are separated by just one atomic mass unit.

Standard pulse counting discrete-dynode electron multipliers have a linear dynamic range extending from a few ions per seconds up to ion count rates of ~$5x10^6$. By using an increased bleed current it is possible to increase this upper linear limit by one order to ~$5x10^7$ cps. But to measure peaks in a mass spectrum which span up to 9 orders of magnitude, it is necessary to extend the dynamic range of a standard electron multiplier detector by around 3 orders of magnitude.

To achieve this extended dynamic range, it is necessary to use a multiplier in analog mode for peaks in the upper 3-4 orders (i.e. for equivalent ion count rates from ~10^6 cps to >10^9 cps), and use the multiplier in pulse-counting mode for ion count rates from 100 to 10^6 cps.

One approach to this problem is to switch the high voltage applied to a standard pulse-counting multiplier in order to switch between analog and pulse-counting modes of operation. The main problem with this approach is that after changing the applied HV when switching modes, the multiplier takes several seconds to settle. This settling delay can interfere with the efficient collection of data. Further, this arrangement can only operate in one of the two modes at any given time.

This article describes a new approach to increasing the effective dynamic range of an electron multiplier by dividing it into two functionally separate sections. The first section of the detector operates in analog mode and is always active, providing a continuous monitor of the ion signal. The second section of the multiplier provides additional gain to the signal and is used in the pulse-counting mode. The pulse-counting section can be rapidly gated off to protect it from very high intensity signal peaks.

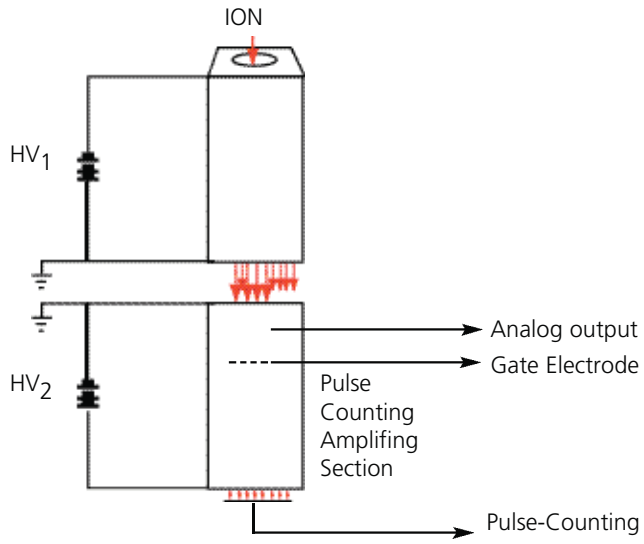

Figure 1 *Schematic diagram showing the functional layout of a 14200 series ACTIVE FILM Multiplier™*

ETP ion detect

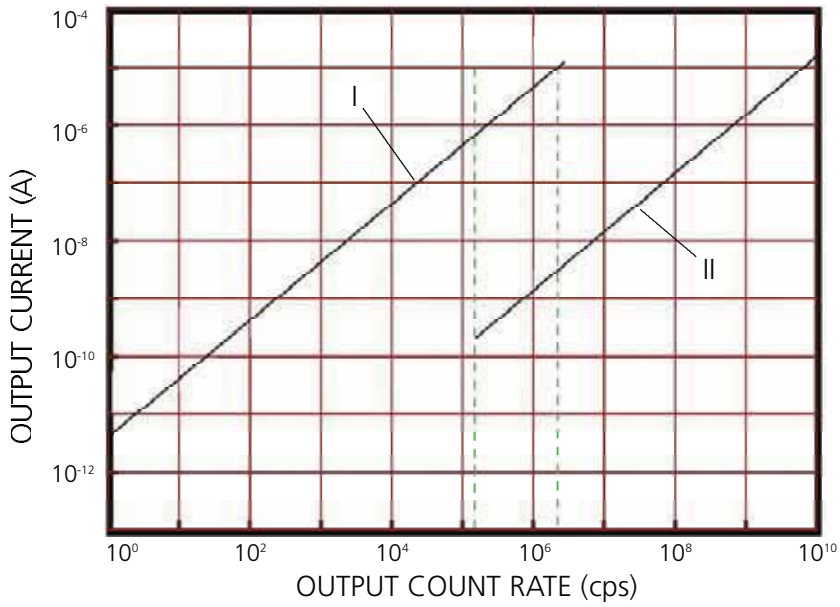

Figure 2 *The curent measured at I the pulse-counting output of the "simultaneous mode" multiplier operated with an overall gain of $3x10^{7}$, and II the analog output multiplier operated with an overall gain of $1x10^{4}$, plotted as a function of the input ion count rate.*

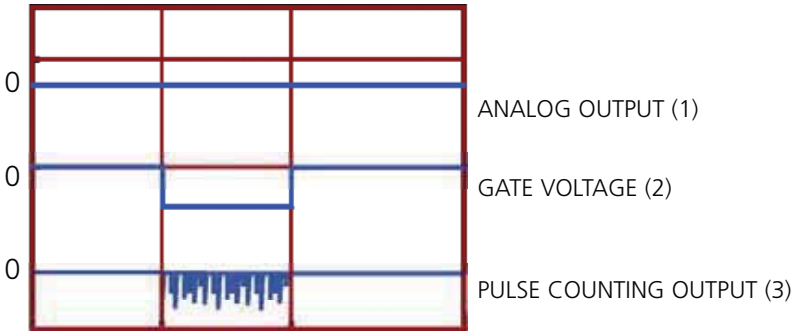

Figure 3 *Effect of the applied gate electrode potential (trace 2) on the analog (trace 1) and pulse counting (trace 3) outputs.*

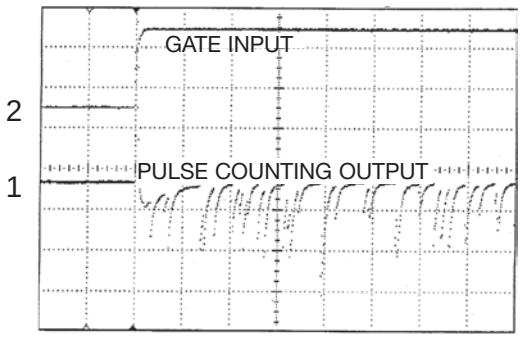

Figure 4 *Oscilloscope trace of the voltage applied to the gate electrode and the corresponding output from the pulse-counting section of a 14200 series simultaneous Mode ACTIVE FILM Multiplier™ (time base is 20µs per division)*

PRINCIPLES OF OPERATION

The 14200 series 'Simultaneous Mode' *ACTIVE FILM Multiplier*™ divides the detector up into two separate amplifying sections, shown schematically in figure 1. The first section of the multiplier operates in analog mode and is operated at a gain of ~$1x10^4$. Following this analog section, a special 'beam-splitting' dynode extracts approximately 50% of the electron signal and directs it into a shielded Faraday Cup from which the analog output signal is taken. The remaining 50% of the electron signal continues on to the pulse-counting section of the multiplier to be further amplified to a level suitable for pulse-counting operation (by another $3x10^3$ making ~$3x10^7$ in total) before being collected by the pulse-counting output electrode.

For operation in analog mode, the gain of the first section of the multiplier is set to ~$1x10^4$. At this gain the correlation between the analog output current and input ion count rate is represented by curve (I) in figure 2. As the maximum linear output current for a discrete-dynode electron multiplier is ~15µA (~15% of the bleed current through the dynode resistor chain for a typical *ACTIVE FILM Multiplier*), then at 10^4 gain this limit corresponds to an equivalent input ion count rate of $5x10^9$ cps.

For operation in pulse-counting mode the gain of second section of the multiplier is set so that the combined gain of both sections of the multiplier is ~$3x10^7$. At this gain the maximum linear count rate of the multiplier (so that its output current is <15µA) is ~$4x10^6$ cps. The correlation between output current and input ion count rate for the pulse-counting section of the multiplier is represented by curve (II) of figure 2.

From the two lines in figure 2 it can be readily seen that when the two modes of operation (analog and pulse-counting) are used in the one detector, the over all linear dynamic range of the detection system would extend from a few ions per second up to >10^9 cps.

At the front end of the pulse-counting section of the multiplier, a special 'Gate' electrode is used to selectively protect the pulse-counting section from exposure to very large peaks.

Figure 3 shows the effect of the potential applied to the gate electrode on both the analog and pulse-counting outputs. When the gate voltage is set to VG (curve 1), the pulse-counting section is enabled and pulses from the input ions are seen from the pulse-counting output (curve 2). At the same time the analog output (curve 3) is also functioning. When the gate is set to ground (0 volts) the pulse-counting section is disabled and there is no output from the pulse-counting section. The operation of the analog output is unaffected by the gate. Consequently, it monitors the ion signal at all times and can be used to select when the lower detection limits of the pulse-counting mode part of the detector are required.

Figure 4 shows an actual oscilloscope trace of the voltage applied to the gate electrode and the corresponding output from the pulse-counting section of the multiplier. A voltage applied to the gate electrode can switch the pulse-counting section "on" or "off" in less than 20µs.

TECHNICAL SPECIFICATIONS

Electrical Parameter	Typical Specification
Application	Quadrupole mass spectrometers
Input ion optics	Off-axis first dynode
Number of lead connections	5
Applied -HV on analog section for 10^4 gain	-1.8 kV
Applied +HV on pulse-counting section for $3x10^7$ gain (assuming 10^4 gain on analog section)	+1.0 kV
Dark current from analog output (-2.5kV)	<1pA
Dark counts from pulse-counting output (+1.8kV/+1.5kV)	0.05 cps
Gate electrode operating voltages	Gate Closed: 0 volts Gate Open: fixed %* of +HV (* varies with specific model)

ETP ion detect

APPLICATION IN MASS SPECTROMETRY

Operation of the pulse-counting part of this detector does not affect the output of the analog section. Consequently the analog output can be used to continuously monitor the ion current from the analyzer. This allows the analog output of the 14200 series *ACTIVE FILM Multiplier* to be used to determine when the pulse-counting section is required and when it should be protected from very high intensity mass peaks.

When the pulse-counting section of the multiplier is activated by application of the appropriate voltage to the gate electrode, the pulse-counting and analog outputs simultaneously give a signal that is proportional to the input ion current and are both valid, provided the maximum count rate of the pulse-counting section is not exceeded.

This continuous monitoring function of the analog output combined with a gated pulse-counting output, makes the 14200 series *ACTIVE FILM Multiplier* ideal for application in fully automated extended dynamic range ion detection systems.

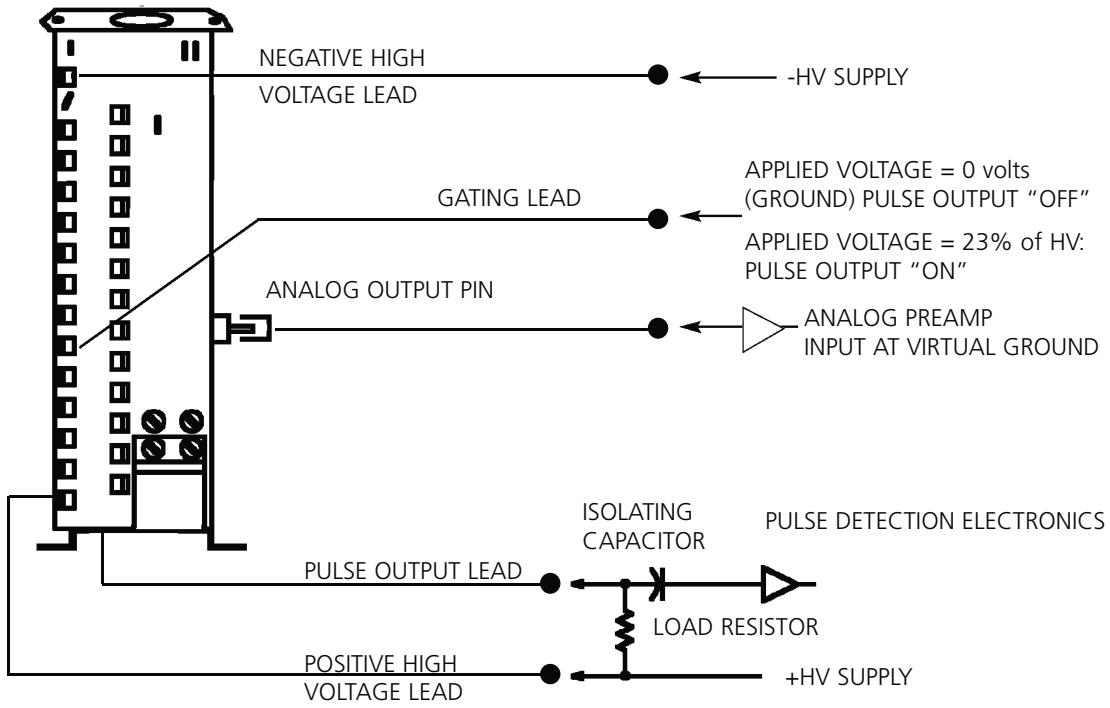

Figure 5 *Wiring diagram for the 14200 series ACIVE FILM Multiplier*

TECHNICAL ARTICLE

ION DETECTION IN ICP-MS USING ACTIVE FILM MULTIPLIER'S™

Kevin Hunter, ETP Scientific, Auburn, MA

Reprinted from Atomic Spectroscopy, Jan/Feb 1994, 17-20

One of the perennial aims of inductively coupled plasma-mass spectrometer (ICP-MS) development is for higher ion sensitivities and lower detection limits. The electron multiplier ion detector plays a key role in determining the overall detection limits that can be achieved by a mass spectrometer, influencing both the ion sensitivity and the background noise levels.

In developing an ACTIVE FILM Multiplier™ specifically for ICP-MS applications, we concentrated our efforts on maximizing the ion signal count rate, while maintaining a very low background count rate. Te result is an electron multiplier capable of ion detection sensitivities that are greatly improved over channel multiplier technology.

In this presentation, the role and electron multiplier plays in an ICP-MS system discussed. A new type of detector called the ACTIVE FILM Multiplier™ is described, detailing what ACTIVE FILM Multiplier™ are, how they work in detecting ions in a mass spectrometer, and finally, how ACTIVE FILM Multiplier's™ perform in an ICP-MS.

ROLE OF THE ELECTRON MULTIPLIER IN AN ICP-MS

Figure 1 shows the functional layout of an ICP-mass spectrometer system. Broadly speaking, the mass spectrometer can be described as having three main sections:

1. The sample introduction system, comprising a liquid sample pumping system that carries the sample to a nebulizer, turning the sample into a fine mist. This mist is then fed into the plasma torch that ionizes the sample producing charged elemental ions. The ions are then introduced into the vacuum system via a set of differentially pumped sampling cones.

2. The quadrupole mass filter separates the ions according to their mass-to-charge ratio.

3. The electron multiplier ion detector detects the ions passed by the quadrupole and produces an amplifying signal that can be processed by the detection electronics before being sent to a computer based data acquisition system.

In order to obtain the highest possible sensitivity from the system, ideally we want the electron multiplier to detect every ion of the selected mass that is passed by the quadrupole mass filter. How efficiently the electron multiplier carries out this task represents a potentially limiting factor on the overall sensitivity of the system. The signal ions exit the quadrupole with a broad spread of exit angles and with kinetic energies up to 25eV. Consequently, the efficient focusing of these ions onto the first dynode of the electron optical design developed for the *ACTIVE FILM Multiplier™* .

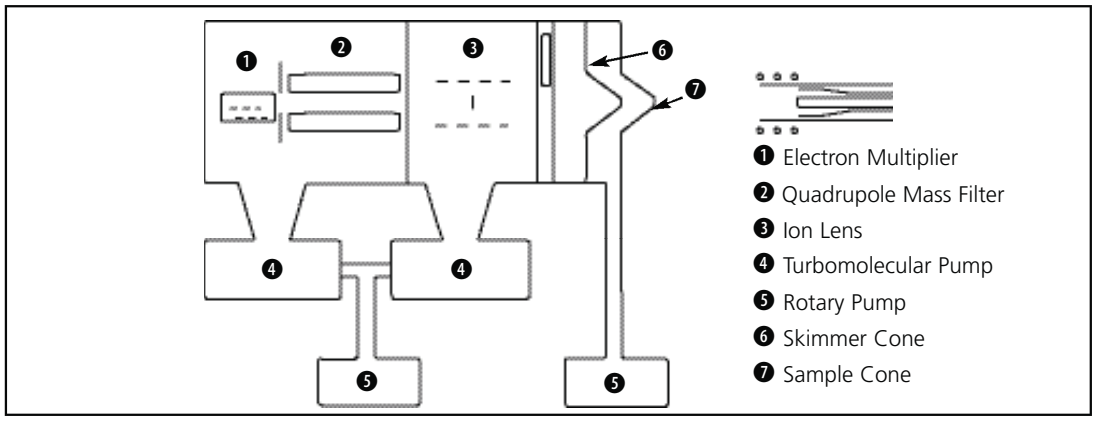

ETP ion detect

ACTIVE FILM MULTIPLIERS™ - PRINCIPLES OF OPERATION

ACTIVE FILM Multiplier's™ are discrete dynode electron multipliers that use an array of up to 21 electrodes, or dynodes, to carry out the electron multiplication process. The name *ACTIVE FILM Multiplier*™ is derived from the multi-layer coating that forms the active area of the dynode surfaces where the electron multiplication takes place.

The surface coating used are a new type of extremel stable - in - air material, which is produced using techniques developed for the semiconductor industry. Repeated or long term exposure to air has no effect on the performance of the multiplier.

Figure 2 illustrates the principles of operation of the discrete dynode electron multiplier. First of all, the general arrangement has an off-axis first dynode, requiring the signal ions from the quadrupole to sweep through a curved path before striking the first dynode. This is done to separate the signal ions from the background noise of neutrals and electromagnetic radiation from the ion source, which pass down the axis of the quadrupole and continue on (missing the first dynode of the multiplier) and are not detected. It is essential to remove this background radiation from the signal to obtain a low background count rate, and hence good signal to noise ratios.

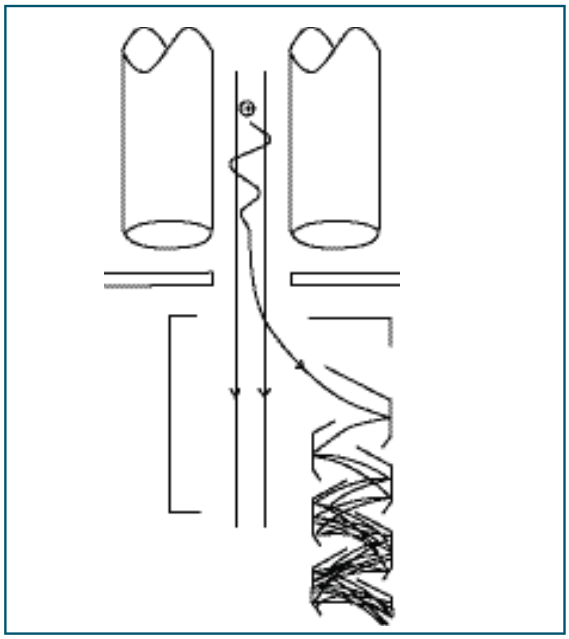

Figure 2. *Optics of an Active Film Multiplier for quadrupole applications*

When a signal ion strikes the first dynode of the multiplier, it liberates secondary electrons. The electron-optics of the dynode design provides for acceleration of these secondary electrons to the next dynode in the multiplier, where they produce more secondary electrons. This process is repeated at each dynode, generating a growing pulse of electrons that are finally captured by the multiplier collector (or anode). The gain of each dynode depends on the energy of the secondary electrons striking its surface and is controlled by the inter-dynode voltage. Thus, by adjusting the high voltage supply, the multiplier can be set to the required gain.

A key element in obtaining the highest possible detection efficiency from a multiplier is focusing as near as possible all the ions from the analyzer onto the first dynode. This involves very careful design of the input ion optics of the multiplier. To tackle this problem, highly specialized electron-optical design software was developed, specifically to handle the design of dynodes in an electron multiplier.

Figure 3 is an output plot from the design software and shows the input optics of a 14500 series *ACTIVE FILM Multiplier*™. The trajectories of ions exiting the quadrupole and being focused onto the first dynode are shown. The dotted lines are euipotential lines spaced at u=intervals of 10% of the high voltage, applied to the first dynode (in this case. HV = 2kV). This pilot clearly shows the very strong lensing effect on the ion trajectories as they pass through the input aperture of the multiplier, bunching the ions together and focusing them onto the first dynode.

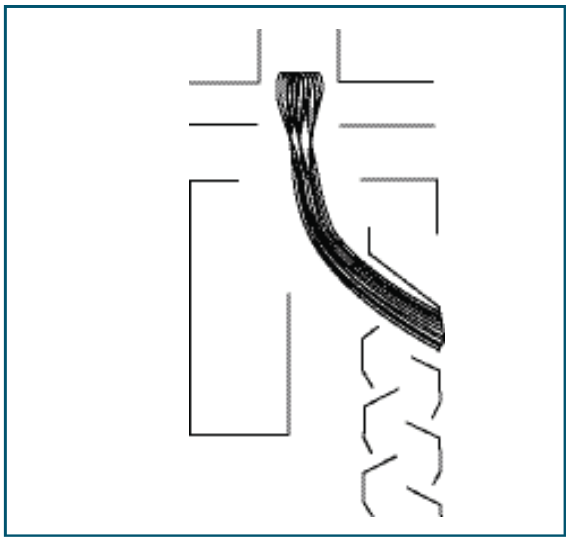

Figure 3. *Computer aided design (CAD) model of input ion optics for positive ions exiting the quadrupole mass filter and being focused onto the first dynode*

Using this kind of plot as a guide, we have been able to produce a design that has a uniformly high ion detection efficiency over the whole area of the multiplier's 11mm diameter aperture. This is demonstrated in figure 4, which shows a three-dimensional plot of the sensitivity (Z axis) of the multiplier over the area of the circular multiplier aperture (X and Y axes). This measurement was taken by scanning the ion beam over the multiplier aperture. This very efficient design of the multiplier input optics is a central element of the higher ion sensitivities that are observed when using this type of multiplier in a mass spectrometer.

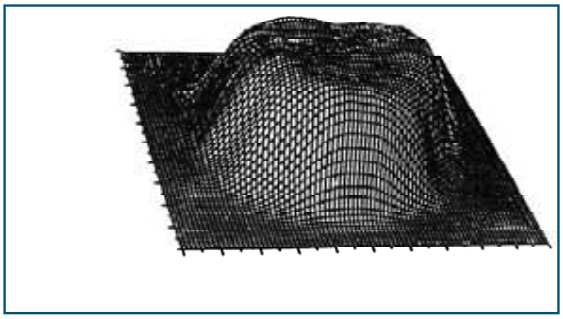

Figure 4. *Plot of the sensitivity over the 11mm diameter aperture of a 14500 series Active Film Multiplier.*

OPERATIONAL CHARACTERISTICS OF ACTIVE FILM MULTIPLIERS™

In ICP-MS applications, where it is required to be able to detect extremely low ion currents, the electron multiplier is normally operated in pulse-counting mode. In this mode, the ion abundance of a mass peak is determined by counting the output pulses from the multiplier for a fixed time interval, with each output pulse corresponding to a single detection ion. This technique allows signals containing only a few tens of ions to be detected.

The operating gain of a pulse counting *ACTIVE FILM Multiplier*™ is usually between 10^6 and 10^8. Figure 5 shows the Gain vs High Voltage curve for a pulse counting *ACTIVE FILM Multiplier*™: the initial operating voltage is typically around 2 kV.

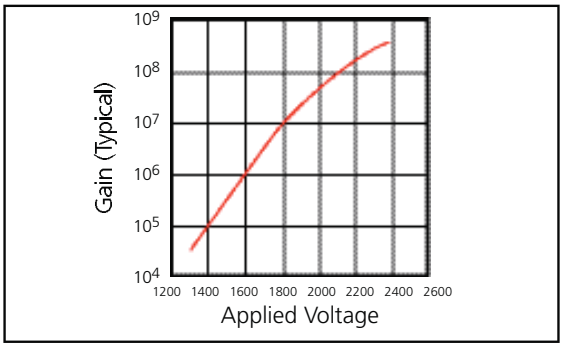

Figure 5. *Gain curve for a pulse counting Active Film Multiplier*

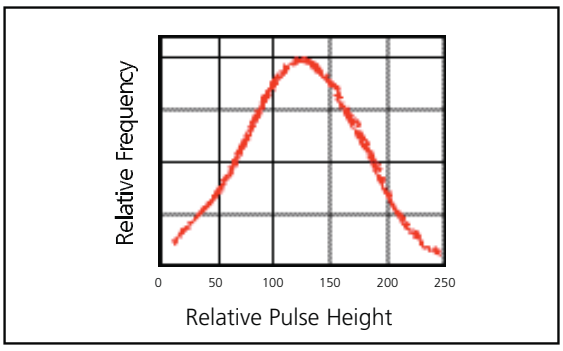

Figure 6. *Output Pulse Height distribution of a pulse counting Active Film Multiplier*

The electron pulses output from the multiplier exhibit a distribution of pulse heights that follow a Gaussian like distribution, as shown in Figure 6. The size of the pulse relates to the total amount of charge contained in the pulse. This type of distribution is usually described in terms of the full-width-at-half-maximum, expressed as a percentage of the distribution peak position (FWHM%).

When a multiplier is set to a given gain, say 10^2, it might be expected that every electron pulse that is output from the multiplier will contain a charge of 10^6 x **e** coulombs, where **e** is the charge on an electron. However, in practice, the charge contained in each pulse output from an electron multiplier varies considerably from pulse to pulse and follows a Gaussian like distribution. The gain at which the multiplier is set really only refers to the average gain of each pulse. The reason for this variation in the pulse sizes from a multiplier resides in the statistical nature of the secondary electron emission process at each of the dynodes.

The secondary electron yield from each dynode, or dynode gain, is determined by the voltage difference between the dynodes. Figure 7a shows the secondary electron yield from a dynode as a function of the energy of the incident electrons which is set by the inter-dynode voltage. If the voltage of the multiplier was set so that the voltage between each dynode is 150 volts, then the gain of each dynode would be 3.6. This means that, on average, 3.6 electrons are emitted from the dynode surface for each incident electron and the number of secondary electrons emitted for each incident primary electron

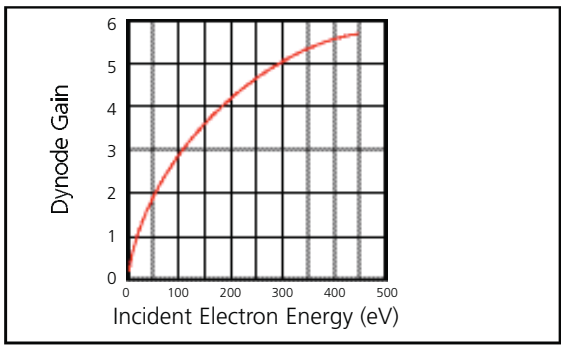

Figure 7a. *Dynode gain plotted against incident electron energy*

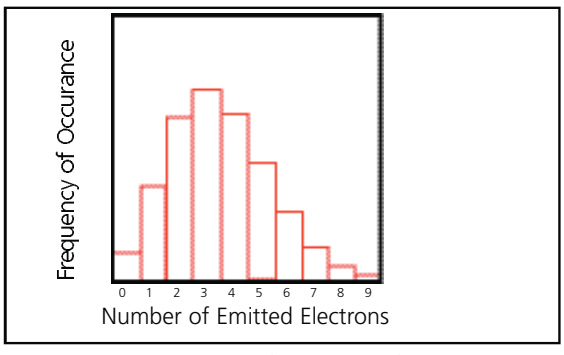

Figure 7b. *Probability distribution for th enumber of emitted secondary electrons per incident electron (mean number of electrons emitted = 3.6)*

follows a Poisson distribution shown in Figure 7b. In this case, sometimes two electrons are emitted, and at other times, three or four electrons are emitted. This statistical variation in the secondary electron emission process at each dynode results in the distribution of pulse sizes measured from the output of the multiplier.

The operating voltage of a pulse counting multiplier is usually set by slowly increasing the high voltage until the output count rate reaches a plateau as described in figure 8. This type of curve is seen because the pulse counting electronics connected to the output of the multiplier only counts those pulses larger than a preset discriminator setting. As the high voltage is increased, the size of the pulses from the multiplier also increases, causing them to cross the discriminator level to be counted and so increase the measured count rate. Eventually, the high voltage is set high enough so that the greater part of the pulse distribution shown in figure 6 is above the discriminator level. At this point, increasing the high voltage is normally set just above the knee on the plateau curve.

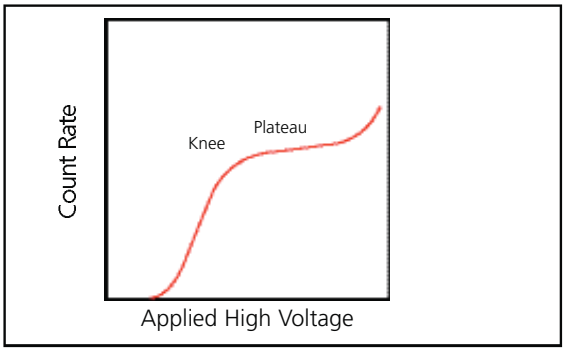

Figure 8. *General form of the pleteau curve for a pulse counting ACTIVE FILM Multiplier™.*

To obtain the longest possible life from an electron multiplier, it is important that the applied voltage be kept to the minimum value that achieves the required performance. Operating a multiplier at higher voltages, and hence higher gains, will shorten its operating life.

Standard pulse-counting *ACTIVE FILM Multiplier's*™ will operate linearly to output count rates up to 5 x 10^6 counts per second. For very high count rates applications, special high count rate models are available that have reduced internal resistance and that will count linearly up to 20 x 10^6 counts per second.

CONCLUSION- PERFORMANCE OF COMMERCIAL ICP-MS INSTRUMENTS

The materials used on the dynode surfaces are very stable. This high stability has two effects on the operation of the multiplier. First the multiplier is stable-in-air, and so repeated or long-term exposure to air has no effect on the performance of the multiplier. Second the multiplier does not require a "burn-in," as is often the case with channel type detectors.

We conducted sensitivity comparison tests in a number of commercial ICP-MS instruments. In this case of the Perkin Elmer Sciex® ELAN™, 5000 increases in the ion sensitivity obtained when using the *ACTIVE FILM Multiplier*™, over that of the previously installed channel-type detector, were consistently between 30% and 100%, without any significant change in the measured background count rate. This translates directly to an improvement in the instrument signal-to-noise. Tests carried out in several Fisions VG Plasmaquad (Fisions Instruments, Winsford, Cheshire, UK) instruments have resulted in similar sensitivity increases.

Field data from ICP-MS instruments using the *ACTIVE FILM Multiplier*™ also indicate that he detector is between 1.5 and 3 times that of the channel-type detector. For example. throughout Australia and Asia, 14 *ACTIVE FILM Multiplier's*™ have recently been installed over a period of 18 months in routine environmental and geochemical laboratories as well as in research institutes. Even though some of these laboratories typically replace traditional continuous-dynode detectors every three to four months, none of the Active Film discrete-dynode detectors needed replacing during this period.

The performance characteristics of the *ACTIVE FILM Multiplier*™ have led to it attaining wide acceptance in mass spectrometry applications, particularly in applications such as ICP-MS, which are very demanding on the detector used. This has resulted in this type of detector being installed as standard in two commercial ICP-mass specrometers. *ACTIVE FILM Multiplier*™ is also gaining increasing acceptance as a replacement detector in the ICP-MS instruments of several other manufacturers.

TECHNICAL ARTICLE

REMOVING DEAD TIME VARIATIONS DUE TO DETECTOR PULSE WIDTH IN ION COUNTING SYSTEMS

Dick Stresau, Kevin Hunter, Wayne Sheils and Peter Raffin
Presented at the 52nd ASMS Conference on Mass Spectrometry and Allied Topics
May 23-27, 2004, Nashville, Tennessee

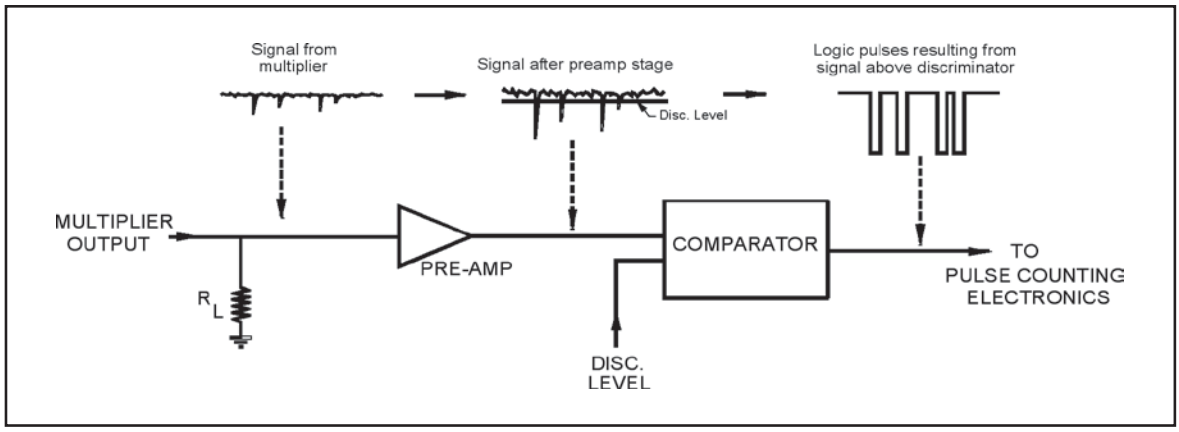

Figure 1. *Schematic diagram of typical ion-counting electronics. This circuit shows pre-amplifier and comparator/discriminator to remove noise from multiplier signal pulses. Note RL can be a separate load resistor but is typically the 50Ω input impedance of the preamp.*

The maximum linear counting rate achievable by a pulse-counting detection system (Figure 1) depends on several parameters:

1. detector linear output current limit
2. detector gain
3. discriminator level, and
4. dead time.

Whereas linear output current and gain are parameters associated with the detector, the discriminator level and dead time are parameters of the supporting electronics.

To achieve the optimum performance from a pulse counting system, it is essential that the discriminator and dead time are appropriate for the characteristics of the detector pulses: If a system dead time far exceeds the detector pulse width, the maximum linear counting rate can be unnecessarily limited by this dead time. (Figure 2) On the other hand, if the pulse width exceeds the dead time, this can cause errors that can not be properly corrected using normal methods.

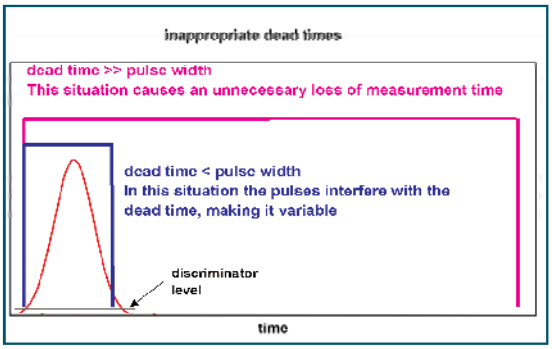

Figure 2. *Two different dead times that are inappropriate for the pulse width illustrated.*

This article addresses this second case, and presents a method for the conditioning of signal pulses from a detector to allow the use of shorter dead times, thereby increasing the maximum achievable counting rate of a system.

ETP ion detect

THE ISSUE

In an MS pulse counting system, count losses occur due to the dead time of the detection system's electronics. The losses that are incurred increase as a function of the rate of ions entering the detection system and the length of the electronic's dead time (Figure 3a). These losses are accounted for by making "dead time corrections" to the measured count rate. For a system with a fixed dead time (ie. a non-paralysable system) the expression relating the true count rate n to the measured count rate m is

$$n = \frac{m}{1 - m\tau} \qquad \ldots\ldots\ldots\ldots\ldots\ldots (1)$$

where τ is the dead time.

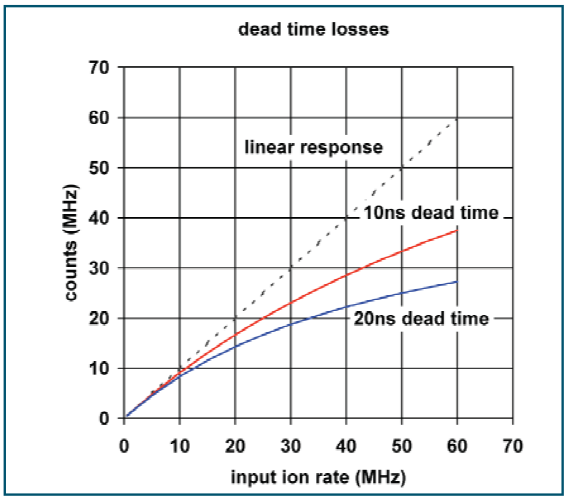

Figure 3a. *The theoretically predicted count rates for detection systems with 10ns and 20ns dead-times. The differences between the predicted count rates and true count rate are due to dead time losses.*

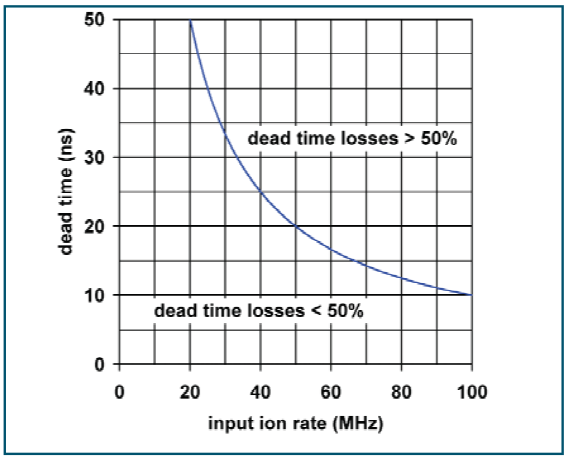

Figure 3b. *The maximum dead time allowed to limit dead time losses to 50% at a given input ion rate.*

To keep corrections accurate, dead time losses are typically limited to ~50%. The dead time required to measure a given true rate while maintaining less than 50% losses is shown in Figure 3b.

Equation 1 describes the correction that applies to a system that has a fixed dead time. To keep the dead time fixed in level-detecting systems (as typically used in MS), the width of the pulse at the discriminator level must be less than the dead time of the electronics.

If the dead time is shorter than the pulse width at the discriminator level, then the dead time can be variable, and Equation 1 is not strictly applicable.

While pulses from an electron multiplier can have a well defined full-width measured at half-height maximum (fwhm), variation in pulse heights can lead to a considerable variation in widths at the fixed level of the discriminator. (Figure 4a). So, it is insufficient that the dead time is longer than the pulse at fwhm, it must be ensured that the dead time is longer than the width of the largest pulses at the discriminator level. (Figure 4b). The output pulses from a standard ETP pulse-counting detector have full-widths at half maximum of ~5ns, but their widths could exceed 20ns at the 5% level.

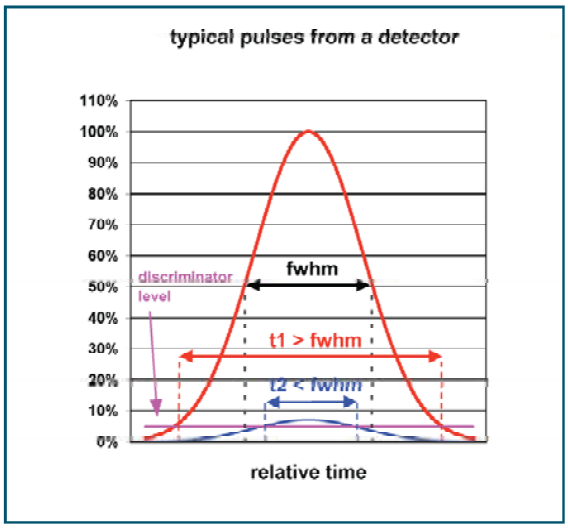

Figure 4a. *Output pulses from a detector have a distribution of pulse heights. While the fwhm of the pulses may have only small variations, the width of the pulses at a fixed discriminator level can have large variations (t1 compared with t2).*

ETP ion detect

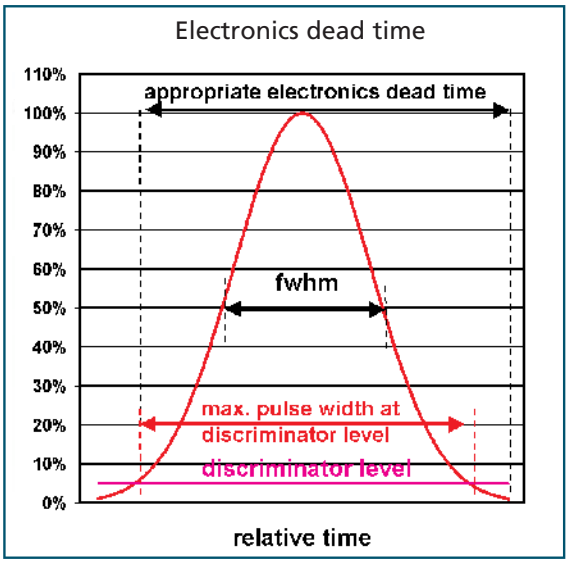

Figure 4b. *The electronics dead time should be set to be longer than the widest pulse at the discriminator level.*

It is worth noting that the dead time is due to the detection system electronics and not the detector - the detector continues to produce output pulses in response to input ions during this dead time, but these output pulses are not recognized by the counting system.

The pulse data shown in Figure 5a were recorded from a special high count rate ETP pulse-counting electron multiplier. Figure 5b shows a set of measurements made with this detector, using an ARI* amplifier/discriminator with an 18ns dead time. This figure also shows the results of applying equation 1 using two different dead times (18ns and 30ns).

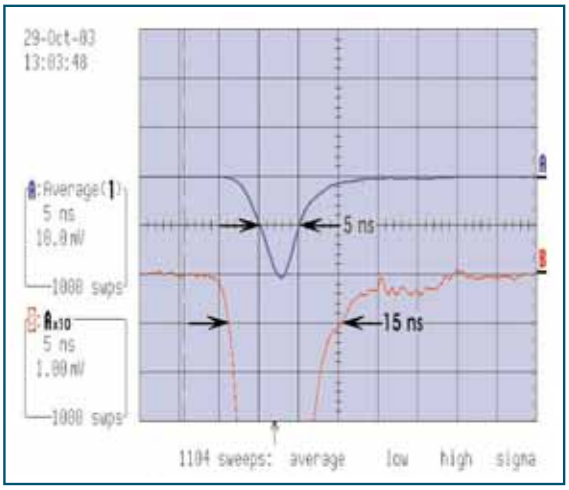

Figure 5a. *Typical pulses from an ETP detector. The average width near the 10mV level (~half-maximum) is ~5ns. The average width near the 1mV level is ~15ns.*

Using a dead time of 30ns gives a better linear correction at higher count rates than does 18ns. This indicates that the system is not behaving as one with a fixed dead time of 18ns, ie. the dead time of the electronics is being affected by the width (at the discriminator level) of the detector pulses.

The work of this project was to investigate if electron multiplier pulses could be processed to provide a narrower pulse width at the discriminator level so
as to remove the interference of the pulses from the electronic's dead time.

**Note:- The amplifier-discriminator used in this work was a model F-100T from Advanced Research Instruments Corporation, 2434 30th Street, Boulder, Colorado. 80301*

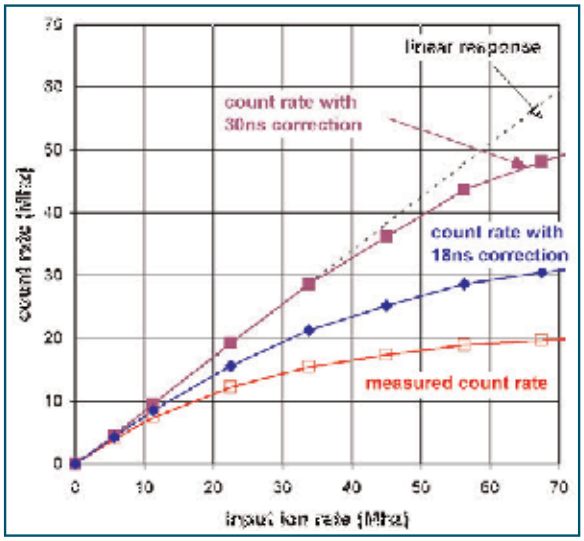

Figure 5b. *Measured and corrected count rates obtained with pulses as shown in Figure 5a. An amplifier/ discriminator with an 18ns dead time was used.*

THE APPROACH

Figure 6a shows an arrangement of a capacitor and resistor that has been introduced into the signal line between a detector and a pre-amp. In this arrangement, these components act as a differentiating circuit.

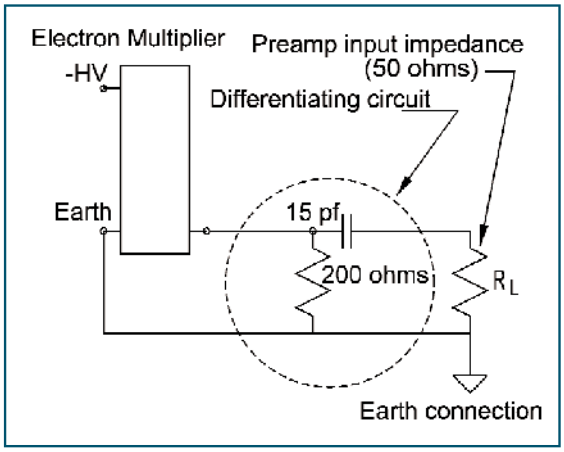

Figure 6a. *An arrangement of a capacitor and resistor that has been introduced into the signal line between a detector and a pre-amp. In this arrangement, these components act as a differentiating circuit.*

The results of a SPICE model of the signal at the pre-amp with and without the differentiating circuit are shown in Figure 6b. The differentiating circuit produces a bipolar pulse that has a rapid return to baseline after it's negative swing, permitting the use of shorter dead times. The differentiated pulse has a smaller negative amplitude than the non-differentiated pulse, requiring the use of a lower discriminator level. However, the differentiating circuit also behaves as a high-pass filter. Together with the low-pass character of the pre-amp input, it forms a notch filter that works to suppress system noise, resulting in an overall improvement of the signal-to-noise ratio.

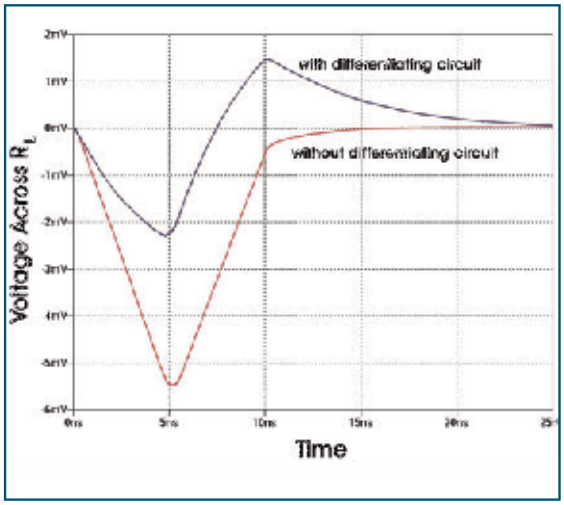

Figure 6b. *The results of a SPICE model of the signal at the pre-amp (R_L) with and without the differentiating circuit.*

By adjusting the R and C values of the circuit, it is possible to tailor the time that the pulse takes to return to baseline from its positive upswing. Since the amplifier-discriminator used in testing had an 18ns dead time, the R and C values chosen were to allow the pulse's re-approach to baseline in this time. (Figure 6b). By choosing different R and C values, this re-approach time could be further reduced for better compatibility to shorter dead times.

RESULTS

Figure 7a shows pulse data recorded from a special high count rate ETP electron multiplier that has been configured to include the differentiating circuit of Figure 6a in its signal line. The pulse shape is seen to be in very good agreement with the SPICE model, with a width of ~ 8ns at the -1mV level, compared with ~15ns for the non-differentiated pulse.

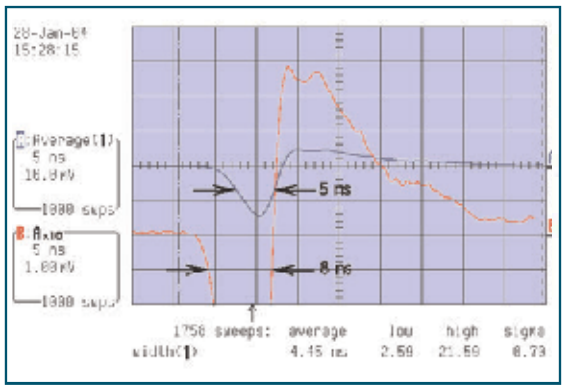

Figure 7a. *Typical pulses resulting from a detector with a differentiating circuit. The average width near the 8mV level (~half-maximum) is ~5ns. The average width near the 1mV level is ~8ns.*

A set of measurements made with this detector is shown in Figure 7b. Applying Equation 1, the correction with best linear fit was obtained by using a dead time of 18ns. In this case, the corrected data shows a linear response out to a count rate of > 50MHz.

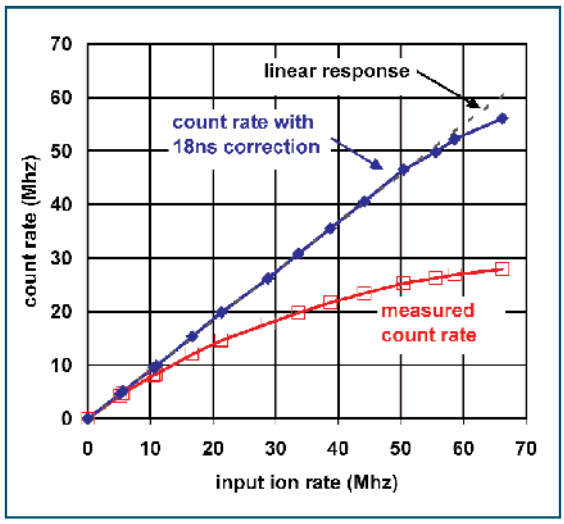

Figure 7b. *Measured and corrected count rates obtained with pulses as shown in Figure 7a. An amplifier/discriminator with an 18ns pulse pair resolution was used.*

This result indicates that the pulses from the detector are not compromising the 18ns dead time of the electronics, allowing a strictly correct use of equation 1. The result is also in agreement with the prediction of Figure 3b that a system with an 18ns dead time has losses of ~ 50% at ~53MHz.

The effect of the circuit on system noise was dramatic. The suppression allowed the discriminator level of the system with which the tests were performed to be set significantly lower than it had ever previously been used (0.5mV).

CONCLUSION

A method for improving the maximum linear count rate of a pulse counting detection system has been demonstrated. The method consists of the introduction of a differentiating circuit into the signal line of an electron multiplier so as to reduce the pulse widths at the discriminator level.

In tests performed, interference with the dead time of the electronics system from detector pulse width was eliminated. Without this interference, the correction that gave the best linear fit to measured data used a dead time that was due entirely to the system electronics, allowing accurate use of the normal dead time correction equation. In this way, corrected count rates were obtained that were linear beyond what has previously been achievable (> 50MHz).

The differentiating circuit also strongly attenuates system noise, allowing the use of significantly lower discriminator levels and operating gain. Therefore, higher count rates will be achieved for a given detector linear output current, and detector life will be enhanced.

The circuit used in this work was tuned to provide the best results for a system with an 18ns dead time. By adjusting component values, the same circuit could be tuned to match systems with any other dead time.

ETP ion detect

TECHNICAL ARTICLE

INFLUENCE OF CAPACITANCE NETWORKS ON THE PULSE DYNAMIC RANGE AND RECOVERY TIME OF TOF DETECTORS

Dick Stresau, Kevin Hunter, Wayne Sheils
Presented at the 50th ASMS Conference on Mass Spectrometry and Allied Topics
June 2-6, 2002, Orlando, Florida

INTRODUCTION

A variety of capacitance networks have previously been used with discrete-dynode multipliers to improve their pulse dynamic range (linear response to high abundance ion peaks). These have been used with some success. In response to demand for even greater dynamic range and recovery time performance, a detailed computer model has been developed, which accurately simulates the mechanisms involved in the pulse response of the detector. This model has been used to investigate the effects of gain suppression and recovery time after high abundance ion bursts and has led to capacitance network designs that improve the pulse dynamic range of a detector by around 2 orders of magnitude.

RESULTS

Figure 1 is a schematic of a basic discrete-dynode electron multiplier showing the dynodes and the resistor chain connecting them. Discrete-dynode multipliers have an inherent small capacitance between the dynodes which has been measured to be ~5pF. When a signal pulse is drawn from the multiplier, the charge removed from each dynode has to be instantly supplied by these small capacitances, which act as reservoirs of charge - the resistor chain is too slow to supply the large instantaneous currents needed. When charge is removed from a dynode by a signal pulse, the voltage across these small capacitances will be changed, and importantly, this will also change the voltages on the dynodes.

Figure 2 is a plot of the voltages between each dynode after different numbers of single ion pulses have been put through the multiplier. The x-axis is the dynode number with 1 being the first dynode and 22 the last dynode, just before the output. Initially (zero ions) the voltage between each dynode is about 77 volts, which is just the applied high voltage divided by the number of dynodes.

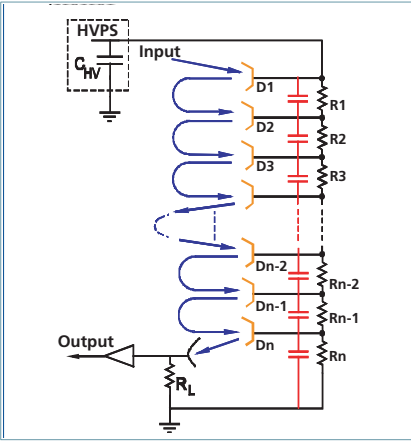

Figure 1. *Schematic of a discrete-dynode multiplier showing the small inter-dynode capacitances.*

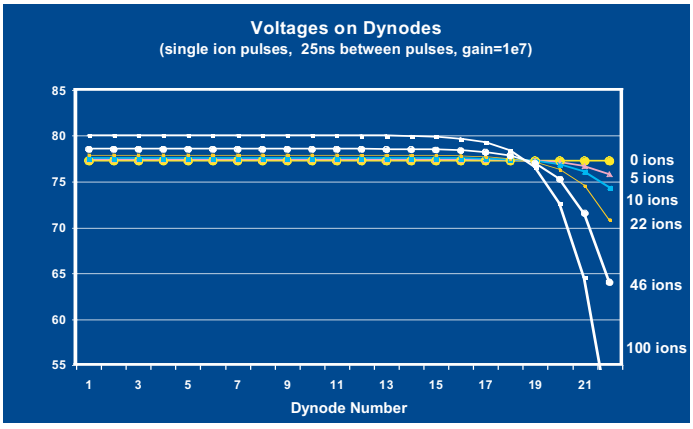

Figure 2. *Change in the voltages between the dynodes of the multiplier. The zero ion line is the initial condition with all the dynodes having equal voltage between them. As single ion pulses pass through the multiplier drawing charge from the capacitors, the voltages between the last few dynodes begin to collapse. This is called saturation.*

ETP ion detect

A very typical layout for a multiplier for high pulse-linearity applications is shown in **Figure 3**, where a number of capacitors have been added to the last few dynodes of the multiplier. In this case we have our standard multiplier circuit with our standard 1.4 megohm resistors between the dynodes and 5nF capacitors are connected between the last 4 dynodes. These capacitors act as very large reservoirs of charge and prevent the voltage on the last 4 dynodes from changing, and so we would expect this to greatly increase the pulse dynamic range of the multiplier.

The modeled response to single ion input is shown in **Figure 4**. As expected, the voltage on the last 4 dynodes does not change. However, something unexpected has happened at the dynode immediately above the capacitors. The voltage on this dynode has now collapsed, and this is now the place where the multiplier becomes saturated. So we have simply moved the problem further up the dynode chain. In this case we are not seeing substantial voltage suppression effects until after about 1000 single ion pulses, compared to ~20 single ion pulses for the case with no added capacitors. ***This is an improvement of about a factor of 50 times.***

If we now add capacitors between ALL the dynodes of the multiplier, we get the result shown in **Figure 5**. In this case, voltage suppression effects are just beginning to be seen on the last dynode after about 20000 single ion pulses have been run through the multiplier. This is a factor of about 1000 times better than the case with no capacitors added to the multiplier, and should result in a major increase in the pulse dynamic-range of a Time-Of-Flight detector. This model has allowed us to design new multipliers with greatly enhanced pulse-dynamic range.

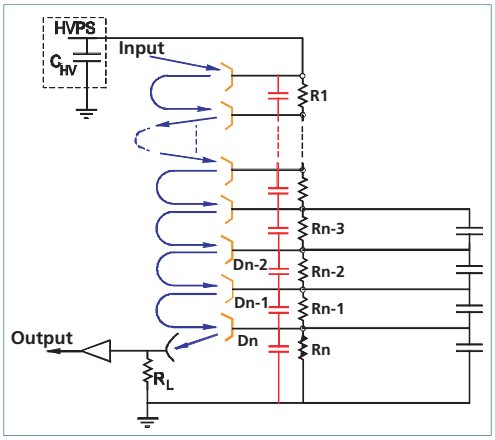

Figure 3. *Schematic of a discrete-dynode multiplier showing the addition of 5nF capacitors on the last four dynodes.*

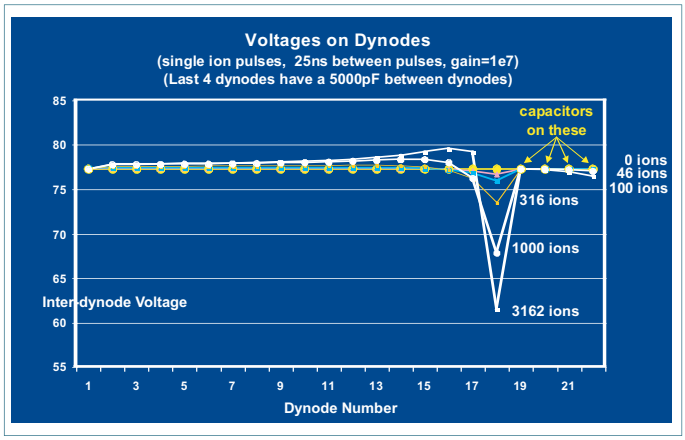

Figure 4. *Change in the voltages between the dynodes of the multiplier shown in Figure 3. Now the voltages on the dynodes with 5nF capacitors attached do not change as charge is removed. Instead the voltage suppression now occurs at the next dynode above the capacitors.*

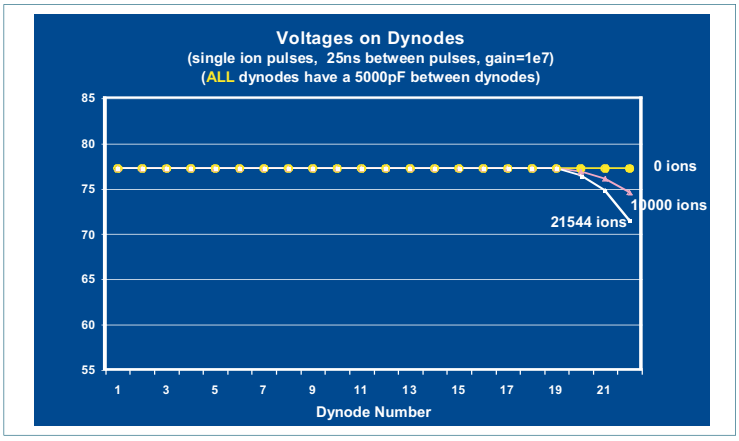

Figure 5. *Change in the voltages between the dynodes of the multiplier with 5nF capacitors connected between all the dynodes. Now the onset of voltage suppression is delayed until after ~20000 single ion pulses. This corresponds to an increase in pulse dynamic range of a factor of ~1000 over the same multiplier with no capacitors attached.*

TECHNICAL ARTICLE

THE "AGING" MECHANISM

IN ELECTRON MULTIPLIERS AND OPERATING LIFE.

Aaron D. Cutter (1), Kevin L. Hunter (2), Peter J. K. Paterson (3) and Richard W. Stresau (1)
1. ETP Electron Multipliers Pty. Ltd., Australia
2. ETP Scientific Inc. Auburn, Massachusetts, USA
3. RMIT Dept. of Applied Physics, Melbourne, Australia
Presented at the 42nd ASMS Conference on Mass Spectroscopy and Allied Topics
May 29-June 3, 1994, Chicago, Illinois

INTRODUCTION

The objective of this study is to determine the primary cause(s) of electron multiplier degradation with use over an extended time, with a view toward optimizing detector lifetime in mass spectrometry applications.

An understanding of the "aging" process in electron multipliers is a necessary precursor to developing a very-long-life mass spectrometer detector. By studying the dynode surfaces of an ETP *ACTIVE FILM Multiplier*™, we have isolated the major factors influencing the deterioration of electron multiplier performance.

Analysis of the dynode surfaces was performed on a discrete-dynode device; however, these results may be generalized for any type of electron multiplier detector.

TEST CONDITIONS & RESULTS

Tests were carried out on a 20-stage *ACTIVE FILM Multiplier*™ operated in a vacuum of $3x10^{-6}$ mbar, pumped by a 'Diffstak' diffusion pump. A constant current of N_2 ions was directed into the multiplier aperture and the multiplier high voltage dynamically adjusted so that its gain was held to a constant $1x10^7$ over the 20 hour test. The multiplier output current was held constant at 25μA.

After accelerated aging for 20 hours, the multiplier was disassembled for analysis. Each dynode of the multiplier was numbered to identify its position in the chain, beginning with the dynode closest to the multiplier input.

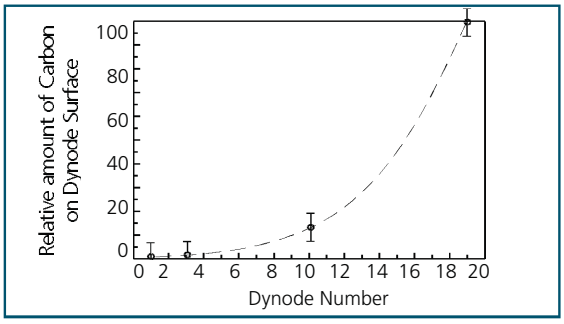

Figure 1 *Relative level of carbon contamination on dynode surfaces (dynode #20: last dynode).*

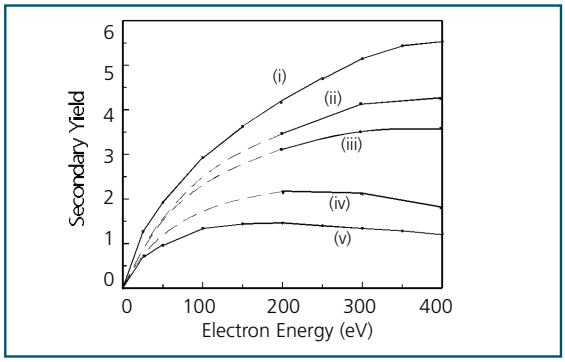

Figure 2 *Secondary electron yield from (i) a new dynode surface of an ACTIVE FILM Multiplier and those of an aged multiplier (ii) dynode 3, (iii) dynode 10, (iv) dynode 19, and (v) the surface of a specially prepared heavily contaminated dynode covered with a very thick carbon layer (for comparison).*

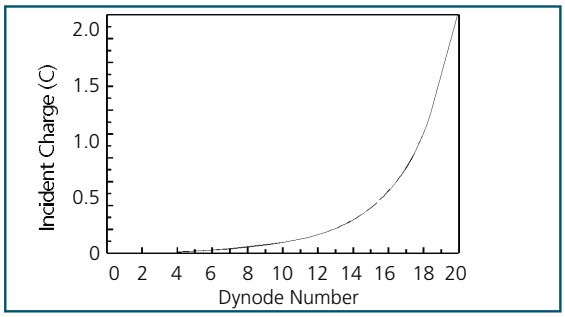

Figure 3 *Theoretical calculation for the total electron dose incident on each dynode.*

Using computer simulation techniques to closely model the operation of a discrete-dynode multiplier, we can estimate the total dose of electrons incident on the surface of each dynode (figure 3).

As would be expected, the dynodes closer to the output of the multiplier are exposed to much greater doses of secondary electrons than those dynodes closer to the input. The shape of the curve in figure 3 is very close to that seen in Figure 1.

ETP ion detect

Analysis of the dynode surfaces was conducted using Auger Electron Spectroscopy (AES). The main contaminant observed on the dynode surfaces was carbon. Contaminant levels increased dramatically on the dynodes nearer to the output end of the multiplier (figure 4).

All the dynodes of the multiplier were exposed to the same environment for the same time interval. The only difference between the dynodes is the dose of secondary electrons they received during the accelerated aging process. This leads us to conclude that the dose per unit area of secondary electrons irradiating the dynode surface is the dominant factor governing the rate at which the dynode surface is contaminated.

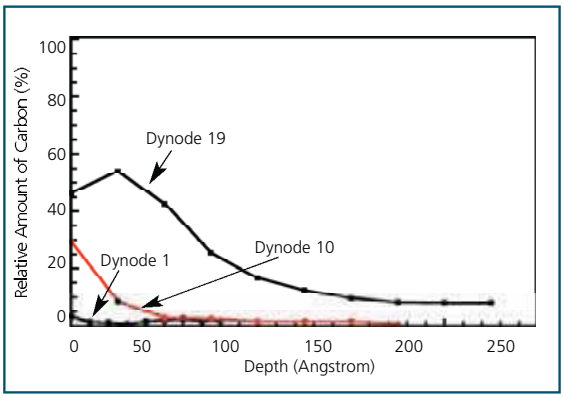

Figure 4 *Depth profiles, taken using Auger Electron Spectroscopy (AES), of the relative amount of carbon contamination on the dynode surfaces of a heavily used multiplier. Dynode 1 corresponds to the first dynode and dynode 19 is the near output.*

CONCLUSIONS

- The amount of carbon deposited is directly related to the total accumulated dose of electrons per unit area on the dynode. (Not simply the time the multiplier is exposed to the environment in the vacuum chamber, even though the vacuum environment plays a major part in determining the overall life of the detector).
- Incident secondary electrons on the dynode surface cause a carbon in the residual gas to become bonded to the dynode surfaces, reducing the secondary yield. (This is a process very similar to electron beam stitching, where the presence of incident electrons is used to facilitate the adhesion of molecules to a surface, and would account for the extreme difficulty of cleaning a contaminated multiplier.) Figure 4 shows a depth profile of the surface layer of a heavily contaminated dynode. Note the oxide layer, still intact, buried beneath a thick layer of carbon contamination.
- Since the process of aging is directly related to the total accumulated charge of electrons per unit area on a dynode surface, an obvious way of increasing the useful life of a multiplier is to increase the surface area of the dynodes. This spreads the electron dose out over a larger area, reducing the accumulated charge per unit area on the dynodes. This is particularly true for the dynodes in the latter third of the dynode chain where the secondary electron currents are much larger.

The increased life of ACTIVE FILM Multipliers™ seen in mass spectrometry applications can in part be attributed to their relatively large surface area (>1000mm^2) compared to 100-150 mm^2 for a standard Channel Electron Multipler (CEM).

ETP Electron Multipliers Pty Ltd
ABN: 35 078 955 521
Address: 8 Martha Street, Clyde NSW 2142 Australia
Tel: +61 (0)2 8876 0100
Fax: +61 (0)2 8876 0199
Email: info@etp-ms.com
Web: www.etp-ms.com